ADHESION AND THE SURFACE ENERGY OF SOLIDS

A dissertation submitted to the

Graduate School of Arts and Sciences
of the University of Cincinnati

in partial fulfillment of the
requirements for the degree of

DOCTOR OF PHILOSOPHY

1954

by

Louis A. Girifalco

B. S. Rutgers University 1950

M. S. University of Cincinnati 1952

ACKNOWLEDGEMENT

The author wishes to express his thanks to Dr. Robert J. Good for help and guidance during the course of this investigation and to Dr. Gerard Kraus for many valuable suggestions. Acknowledgement is also extended to Donald Paynter for performing a major portion of the calorimetric measurements.

This work was performed under Army Air Force Contract AF 33 (616) 231.

Abstract

of

ADHESION AND THE SURFACE ENERGY OF SOLIDS

A dissertation submitted to the

Graduate School of Arts and Sciences
of the University of Cincinnati

in partial fulfillment of the
requirements for the degree of

DOCTOR OF PHILOSOPHY

1954

by

Louis A. Girifalco

B. S. Rutgers University 1950

M. S. University of Cincinnati 1952

TABLE OF CONTENTS

INTRODUCTION

In order to separate two phases in direct contact with each other, a force must be applied, and energy supplied to the system. The forces responsible for the adhesion of two phases are of the same type as those involved in condensation and cohesion phenomena; that is, the intermolecular forces of attraction.

The central problem of adhesion is the experimental determination and theoretical calculation of the force and energy of adhesion. Thus far, theoretical calculations for the force of adhesion have been largely unsuccessful, and the energy of adhesion can be computed for only the simplest of systems, as for example, graphite in contact with carbon tetrachloride[1], and even in these cases the error may be large. There are several reasons for this unsatisfactory situation. First, present knowledge of intermolecular forces is simply not extensive enough to deal with molecules that are not spherical and do not interact predominantly through dispersion forces. Second, very little is known about the molecular-kinetic structure of interfaces, and since an overwhelming percentage of interaction between two adhering phases takes place in the immediate region of the interface, this is a serious handicap. Finally, real interfaces possess cracks, flaws, and irregularities that may be serious enough

to completely control the properties of the adhering system.

The thermodynamic functions of adhesion for liquid-liquid systems can be obtained from surface and interfacial tension data, and for solid-liquid systems from heats of wetting and works of adhesion. No method of measurement has yet been given for solid-solid systems. This is unfortunate since most of the adhesive systems of interest found in practice are of the solid-solid type.

Some progress, however, can be made in the solid-solid adhesion problem. This paper reports an attempt to obtain energies of adhesion and cohesion from heat of wetting and adsorption data, using an approximate theory based on the Fowler and Guggenheim integrals[2] for the adhesion energy. The method essentially resolves itself into determining the surface and interfacial energies of solids.

Because of the pronounced heterogeneity of most surfaces and interfaces, the energies thus obtained are average values and do not give a complete description of the surface energetics. To completely characterize a surface, the distribution function for the surface energy, i.e., the fraction of the surface having energy greater than any specified value, as well as the average surface energy, must be known.

An experimental technique has been developed from which the distribution function can be evaluated. The theo-

retical basis of the method is the definition of the mean and the approximate theory from the Fowler-Guggenheim integrals.

In applying the theory to the measurement of the adhesion energy of ice to various solids, it was found possible to cancel out approximations due to simplifying assumptions by using adsorption data. The adhesion energy thus calculated is limited largely by the accuracy of the experiments rather than of the theory.

Although the primary purpose of this work is the elucidation of some adhesion phenomena, the theory leads to a set of mathematical relations between other surface quantities. These relations were explored in testing the theory.

THEORETICAL DEVELOPMENT. I. FUNDAMENTALS

I. Thermodynamics of Adhesion

The definitions of the thermodynamic functions of adhesion given in this section are essentially those of Harkins[3] with some changes in notation and emphasis so as to present a logical structure consistent with the purpose of this work.

The process of adhesive failure may be schematically represented as follows:

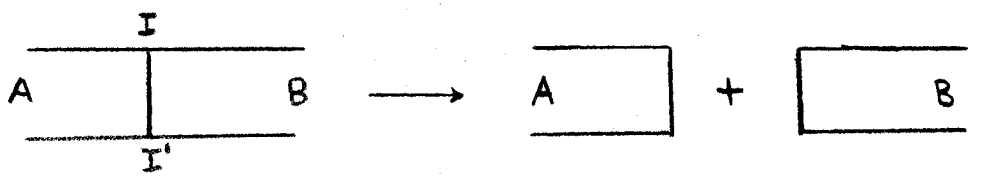

(1)

In this process two phases A and B, in contact across an interface II', are separated to give two phases removed an infinite distance from each other, each phase having its own surface with no trace of any other material adsorbed on it. The process can also be written symbolically as:

$$A/B \longrightarrow A/ + B/ \qquad (2)$$

where A/B represents the adhering system, A/ represents phase A with its own surface, and B/ represents phase B with its own surface.

The only difference between the initial and final states in the adhesive failure process, is that the interface

between the two phases has been replaced by the two free surfaces. Thus if

ϵ_a = surface energy of A per cm.^{2}

ϵ_b = surface energy of B per cm.^{2}

ϵ_{ab} = energy of the A/B interface per cm.^{2}

then the energy of adhesive failure per cm.^{2} of interface may be defined as

$$\Delta E^a_{ab} = \epsilon_a + \epsilon_b - \epsilon_{ab} \qquad (3)$$

$-\Delta E^d_{ab}$ is the energy of adhesion of A to B per cm.^{2} of adhering interface.

Similarly the free energy of adhesive failure per cm.^{2}, ΔF^a_{ab} is given by

$$\Delta F^d_{ab} = \gamma_a + \gamma_b - \gamma_{ab} \qquad (4)$$

γ_a = surface free energy of A per cm.^{2}

γ_b = surface free energy of B per cm.^{2}

γ_{ab} = interfacial free energy of A in contact with B per cm.^{2}

Also, the entropy of adhesive failure is

$$\Delta S^d_{ab} = S_a + S_b - S_{ab} \qquad (5)$$

If both phases are the same, the process represented by (1) is that of cohesive failure and equations (3),

(4), and (5) become the energy, free energy, and entropy of cohesive failure. Writing these for phase A,

$$\Delta E_a^c = 2\epsilon_a \qquad (3')$$

$$\Delta F_a^c = 2\gamma_a \qquad (4')$$

$$\Delta S_a^c = 2S_a \qquad (5')$$

Similarly for phase B,

$$\Delta E_b^c = 2\epsilon_b \qquad (3'')$$

$$\Delta F_b^c = 2\gamma_b \qquad (4'')$$

$$\Delta S_b^c = 2S_b \qquad (5'')$$

These equations result from equations (3), (4), and (5) when both phases are the same, since there is no interface between phases A and B.

When both phases are liquid, no difficulty at all is met in obtaining the thermodynamic functions of adhesion. All the surface and interfacial properties are readily available from surface and interfacial tension measurements.

If one phase is liquid and the other phase solid, the adhesion functions can still be obtained from heat of wetting and work of adhesion measurements. When a solid is immersed in a bulk liquid, the process is one of destroying a solid surface and creating a solid-liquid interface. The

energy liberated is called the heat of wetting and may be written as follows:

$$\Delta H_w = \epsilon_{SL} - \epsilon_S \tag{6}$$

ΔH_w = heat of wetting per cm.^{2}

ϵ_{SL} = energy of the solid-liquid interface per cm.^{2}

ϵ_S = energy of the solid surface per cm.^{2}

Equation (3) for the solid-liquid case becomes

$$\Delta E^a_{SL} = \epsilon_S + \epsilon_L - \epsilon_{SL} \tag{7}$$

where ϵ_L = energy of the liquid surface per cm.^{2}. Combining (6) and (7) gives

$$\Delta E^a_{SL} = \epsilon_L - \Delta H_w \tag{8}$$

Since the heat of wetting can be measured calorimetrically, the energy of adhesion of a liquid to a solid can be determined.

Equation (4) for the free energy of adhesion applied to a solid-liquid system becomes

$$\Delta F^a_{SL} = \gamma_S + \gamma_L - \gamma_{SL} \tag{9}$$

From Young's equation,

$$\gamma_{SL} = \gamma_{SV} - \gamma_L \cos\theta \tag{10}$$

where θ is the contact angle of the liquid with the solid and γ_{sv} is the surface free energy of the solid when in equilibrium with the saturated vapor of the liquid. The quantity $(\gamma_s - \gamma_{sv})$ is the equilibrium film pressure π_e and can be obtained from adsorption isotherms using the relation given by Bangham[4,5,6] based on the Gibbs adsorption isotherm.

$$\gamma_s - \gamma_{sv} \equiv \pi_e = \frac{RT}{V\Sigma} \int_0^{p_0} \frac{v}{p}\, dp \qquad (11)$$

In this equation, R is the gas constant, T the absolute temperature, V the molar volume of gas, Σ the specific surface area of the solid, p the equilibrium pressure of the adsorbed gas, v the volume at S.T.P. of gas adsorbed per gram of solid, and p_0 the equilibrium vapor pressure of the adsorbate at the temperature T.

Combining (9) and (10),

$$\Delta F_{sl}^{s} = (\gamma_s - \gamma_{sv}) + \gamma_l (1 + \cos\theta)$$

or since $\gamma_s - \gamma_{sv} = \pi_e$,

$$\Delta F_{sl}^{s} = \pi_e + \gamma_l (1 + \cos\theta) \qquad (12)$$

This treatment assumes the solid to be insoluble in the liquid so that γ_l is not affected by the presence of the solid. Thus the free energy of adhesion of a liquid to a solid can be determined since π_e, γ_l and $\cos\theta$ are experi-

mentally measurable quantities.

None of these methods are applicable to determining the energy or free energy of adhesion for solid-solid systems. Before describing the method for obtaining surface and interfacial energies for solids, and therefore the energies of adhesion, the relation between the energy of adhesion and of adsorption will be summarized.

A two-phase adhesive system may be formed by the adsorption of one phase onto the other from the vapor state. If the adsorbed layer is a "duple film", i.e., is sufficiently thick so that its free surface has the same properties it would have if the substrate were not present, the final system would be the same as the adhesive system of equation (1). The adsorption of vapor on a substrate may be considered as occurring in three hypothetical steps as follows:

1. Condense the vapor to the bulk phase (liquid or solid depending on the temperature)
2. Extend the bulk phase into a film of the same area as the substrate
3. Adhere this film to the substrate

The overall energy change is the heat of adsorption of the film, Q_a. In terms of the above three steps the heat of adsorption of the film is

$$Q_a = Q_s - 2\epsilon_a\Sigma + \Delta E^a_{ab}\Sigma \qquad (13)$$

Q_s = energy of condensation of the vapor to the bulk phase A

ϵ_a = surface energy of phase A

ΔE^a_{ab} = energy of adhesion of phase A to the substrate phase B

Σ = surface area of the substrate

Solving for the energy of adhesion,

$$\Delta E^a_{ab} = \frac{(Q_a - Q_s)}{\Sigma} + 2\epsilon_a \qquad (14)$$

The quantity $(Q_a - Q_s)$ is the net heat of adsorption of A on substrate B, over the energy of condensation for the entire film made up of n moles of phase A. In terms of the differential heat of adsorption $(Q_a - Q_s)$ is

$$Q_a - Q_s = \int_0^\infty (q_a - q_s)\, dn \qquad (15)$$

In this equation, q_a is the differential heat of adsorption per mole of A on B and q_s is the heat of vaporization per mole of A. As n increases, q_a approaches q_s so that the integrand is zero after a finite value of n.

q_a can be measured isosterically by obtaining adsorption isotherms at two or more different temperatures and picking off points of equal adsorption. The differential heat of adsorption can then be calculated from an equation of Clausius-Clopeyron type[7] for the particular amount ad-

sorbed.

$$\left(\frac{\partial \ln p}{\partial T}\right)_n = \frac{q_a}{RT^2} \qquad (16)$$

p = pressure at n moles adsorbed.

In the integrated form at two different temperatures T_1 and T_2 this is

$$q_{a(n)} = 2.303\, R \frac{T_1 T_2}{T_2 - T_1} \left(\log \frac{p_2}{p_1}\right)_{n = \text{CONST.}} \qquad (17)$$

p_2 = pressure when n moles are adsorbed at T_2

p_1 = pressure when n moles are adsorbed at T_1

Thus the energy of adhesion can be measured by this method provided that one of the phases is volatile enough to permit the determination of adsorption isotherms, and provided that the surface energy of the adsorbed phase is known. The method has been applied to the measurement of the adhesion energy of ice to several solids, using surface energy values obtained from heat of wetting measurements and the theory based on the Fowler and Guggenheim integrals. The details of this work will be given in a later section.

II. Molecular Forces and Adhesion

As shown by equations (7) through (12) both the energy and free energy of adhesion are measurable quantities for solid-liquid systems. From equations (7) and (9)

$$\epsilon_S - \epsilon_{SL} = \Delta E^a_{SL} - \epsilon_L \tag{18}$$

$$\gamma_S - \gamma_{SL} = \Delta F^a_{SL} - \gamma_L \tag{19}$$

In these equations, ΔE^a_{SL}, ΔF^a_{SL}, ϵ_L and γ_L are known or can be measured. Thus if ϵ_{SL} can be expressed as a function of ϵ_S and ϵ_L, ϵ_S can be calculated. Similarly, if γ_{SL} can be found in terms of γ_S and γ_S, γ_S can be calculated. The problem is to compute interfacial properties from surface properties; i.e., functions of the following type are desired:

$$\gamma_{ab} = f(\gamma_a, \gamma_b) \tag{20}$$

$$\epsilon_{ab} = g(\epsilon_a, \epsilon_b) \tag{21}$$

The restrictions imposed on these functions by the physical situation can be listed. From general considerations it is evident that equation (20) must be subject to the following conditions:

1. The function $f(\gamma_a, \gamma_b)$ must be symmetrical in γ_a and γ_b.
2. The value of γ_{ab} is usually between that of γ_a and γ_b because the force field of a free surface

is in general more unsaturated than the force field of an interface.

3. As $\gamma_a \longrightarrow 0$, $\gamma_{ab} \longrightarrow \gamma_b$

4. As $\gamma_b \longrightarrow 0$ $\gamma_{ab} \longrightarrow \gamma_a$

5. As $\gamma_a \longrightarrow \infty$ $\gamma_{ab} \longrightarrow \infty$

6. As $\gamma_b \longrightarrow \infty$ $\gamma_{ab} \longrightarrow \infty$

An exactly similar set of conditions must hold for equation (21) in terms of the ϵ's instead of the γ's.

Equations satisfying these requirements can be obtained as follows:

When two phases approach each other, the molecules of one phase exert forces on the molecules of the other. These forces are the source of the thermodynamic functions of adhesion. Consider two phases A and B, with plane surfaces of equal area that are parallel to each other and a distance z apart (Figure I).

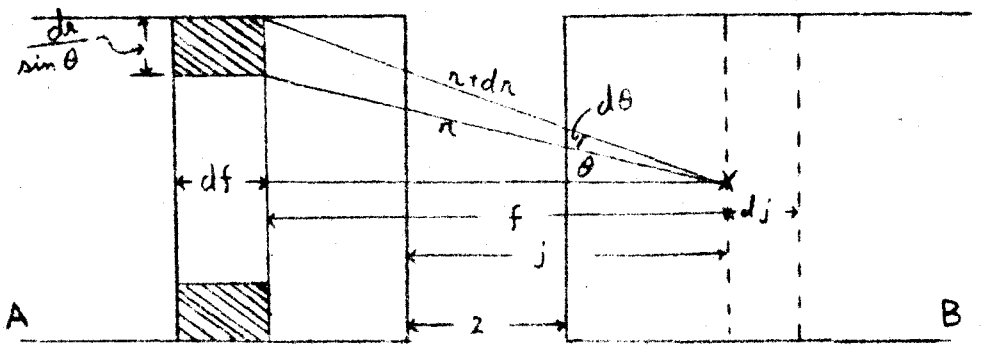

Figure I

Take a particular molecule at a point X in phase B, at a distance f from a slab of thickness df in phase A. The

slab df is parallel to the surfaces of A and B. From this slab, trace out an annular ring whose inner and outer circumferences, on the side closest to X, are at distances r and r + dr from the molecule at X. Figure I shows that the annular ring has a radius of r sin θ and width $\frac{dr}{\sin \theta}$, so that its volume is

$$2\pi r\, dr\, df$$

Let $\varepsilon_{ab}(r)$ be the energy of interaction between a molecule of type A and one of type B, and let η_a be the average number of molecules per cm.^{3} in the annular ring of phase A. Then the interaction energy between molecule X and all the molecules in the annular ring is

$$2\pi \eta_a \varepsilon_{ab}(r)\, r\, dr\, df$$

The interaction energy of molecule X with the entire df slab is obtained by integrating this expression over r from f to oo; thus:

$$2\pi\, df \int_f^\infty \eta_a \varepsilon_{ab}\, r\, dr$$

If j is the distance from X to the surface of phase A, integration over f from j to oo gives the interaction energy between molecule X and the semi-infinite molecule of phase A;

$$2\pi \int_j^\infty df \int_f^\infty \eta_a \varepsilon_{ab}\, r\, dr$$

Now take a slab of thickness dj in phase B whose surface nearest phase A goes through molecule X, and is parallel to the surfaces of A and B. Let n_b be the number of molecules per cm.^{3} in the dj slab. Then the interaction energy between the dj slab and the semi-infinite volume of phase A is

$$2\pi\Sigma n_b\, dj \int_j^\infty df \int_f^\infty n_a \varepsilon_{ab}\, r\, dr$$

where Σ is the area of the surface of phase A or of phase B.

The interaction energy of all of phase A with all of phase B is derived by integrating over j from z to infinity which gives

$$2\pi\Sigma \int_z^\infty n_b\, dj \int_j^\infty df \int_f^\infty n_a \varepsilon_{ab}\, r\, dr$$

Call this energy of interaction $\Delta E^a_{ab}(z)$ per cm.^{2}. Then, dividing the triple integral by the surface area so as to express it per unit area,

$$\Delta E^a_{ab}(z) = 2\pi \int_z^\infty n_b\, dj \int_j^\infty df \int_f^\infty n_a \varepsilon_{ab}\, r\, dr \qquad (22)$$

Equation (22) gives the energy required to separate two phases from a distance z to an infinite distance apart. When z = o, this is the energy of adhesive failure discussed in the preceding section, i.e.,

$$\Delta E^{a}_{ab}(z=0) = \Delta E^{a}_{ab}(0) = \Delta E^{a}_{ab}$$

Since force is the gradient of a potential, the magnitude of the force acting between molecule X and the molecules in the annular ring, in a direction perpendicular to the plane of the ring, is

$$n_a 2\pi r \frac{f}{r} \frac{\partial \mathcal{E}_{ab}}{\partial r} dr\, df = 2\pi n_a f \frac{\partial \mathcal{E}_{ab}}{\partial r} dr\, df$$

The force acting between molecule X and the df slab is

$$2\pi f df \int_f^\infty n_a \frac{\partial \mathcal{E}_{ab}}{\partial r} dr$$

and the force between the X molecule and the semi-infinite volume of A is

$$2\pi \int_j^\infty f df \int_f^\infty n_a \frac{\partial \mathcal{E}_{ab}}{\partial r} dr$$

Multiplying by $n_b dj\sum$, the number of molecules in the dj slab, gives the force acting between the dj slab and the semi-infinite volume of A. This is

$$2\pi n_b \Sigma \, dj \int_j^\infty f\,df \int_f^\infty n_a \frac{\partial \mathcal{E}_{ab}}{\partial r}\, dr$$

Integrating this expression over j from z to infinity gives the force acting between the two phases when their surfaces are a distance z apart. Reduced to unit area, this force is

$$\mathcal{F}_{ab}^{a}(z) = 2\pi \int_z^\infty n_b\, dj \int_j^\infty f\,df \int_f^\infty n_a \frac{\partial \mathcal{E}_{ab}}{\partial r}\, dr \qquad (23)$$

To get the free energy of adhesion as a function of separation distance, simply integrate the force as given by (23) from the distance of separation to infinity. Thus if $\Delta F_{ab}^{a}(z)$ is the free energy of adhesion when A and B are distance z apart,

$$\Delta F_{ab}^{a}(z) = 2\pi \int_z^\infty d\chi \int_\chi^\infty n_b\, dj \int_j^\infty f\,df \int_f^\infty n_a \frac{\partial \mathcal{E}_{ab}}{\partial r}\, dr \qquad (24)$$

Equations (22), (23), and (24) were given by Fowler and Guggenheim, and represent the energy, force and free energy required to separate two phases from a distance z apart, to an infinite distance apart, in terms of the intermolecular potential function $\mathcal{E}_{ab}$. If $\mathcal{E}_{ab}$, n_a and n_b were known exactly, the required energy, force, and free energy

could be directly calculated. For simple systems, n_a and n_b, the "microscopic densities", could be approximated from radial distribution functions and bulk densities, and ε_{ab} could be obtained. In general, however, none of these functions are known with any accuracy so that the results would be only approximate. In any case, a separate set of long and involved calculations would be required for each system. However, relations of the form of (20) and (21) can be obtained by expressing the adhesion functions in terms of the cohesion functions, which, although not exact, are of general applicability.

It is well to note at this point that equations (22), (23), and (24) themselves are not exact since they assume planar, homogeneous surfaces and that the molecules in the surface are in a state not very different from molecules in the bulk phase.

In order to get usable formulae, an idealized model must be set up that enables the integrals to be evaluated or eliminated. The model chosen in this work is embodied in two assumptions:

1. n_a and n_b are constants. This amounts to assuming that the molecular density is constant up to a geometrical plane, where there is a sharp discontinuity.

2. The intermolecular potential function is given by the Lennard-Jones 6-m equation[8] as

$$\varepsilon_{ab} = -\frac{A_{ab}}{r^6} + \frac{B_{ab}}{r^m} \tag{25}$$

A_{ab} and B_{ab} are constants.

The constant B_{ab} can be eliminated from (25) by determining the equilibrium distance between a molecule of A and one of B. Thus, differentiating (25) gives the force acting between two molecules.

$$\frac{\partial \varepsilon_{ab}}{\partial r} = \frac{6 A_{ab}}{r^7} - \frac{m B_{ab}}{r^{m+1}} \tag{26}$$

At the equilibrium distance between the two molecules, d_{ab}, the total force is zero. Therefore at $r = d_{ab}$

$$\frac{6 A_{ab}}{d_{ab}^7} = \frac{m B_{ab}}{d_{ab}^{m+1}}$$

so that

$$B_{ab} = \frac{6}{m} A_{ab} d_{ab}^{m-6} \tag{27}$$

Using (27), equations (25) and (26) can be written,

$$\varepsilon_{ab} = -A_{ab}\left[\frac{1}{r^6} - \frac{6 d_{ab}^{m-6}}{m r^m}\right] \tag{28}$$

$$\frac{\partial \varepsilon_{ab}}{\partial r} = 6 A_{ab}\left[\frac{1}{r^7} - \frac{d_{ab}^{m-6}}{r^{m+1}}\right] \tag{29}$$

III. The Relation between the Adhesion and the Cohesion Energies.

Putting (28) into (22), and using the assumption that n_a and n_b are constants,

$$\Delta E_{ab}^{a}(z) = 2\pi n_a n_b A_{ab} \int_z^\infty dj \int_j^\infty df \int_f^\infty \left[\frac{1}{r^5} - \frac{6 d_{ab}^{m-6}}{m r^{m-1}} \right] dr \qquad (30)$$

To get d_{ab} out of the integral sign, make the change of variable from r to y such that

$$y = \frac{r}{d_{ab}} \qquad \text{so that}$$

$$r = y d_{ab} \qquad \text{and} \qquad dr = d_{ab}\, dy \qquad (31)$$

Then (30) becomes

$$\Delta E_{ab}^{a}(z) = 2\pi n_a n_b A_{ab} \int_z^\infty dj \int_j^\infty df \int_f^\infty \left[\frac{1}{y^5 d_{ab}^5} - \frac{6}{m y^{m-1} d_{ab}^5} \right] d_{ab}\, dy \qquad (32)$$

Taking out the d_{ab} terms,

$$\Delta E_{ab}^{a}(z) = \frac{2\pi n_a n_b A_{ab}}{d_{ab}^4} \int_z^\infty dj \int_j^\infty df \int_f^\infty \left[\frac{1}{y^5} - \frac{6}{m y^{m-1}} \right] dy \qquad (33)$$

In both phases are the same, the energy of adhesion $\Delta E^{a}_{ab}(z)$ becomes the energy of cohesion $\Delta E^{c}_{a}(z)$ or $\Delta E^{c}_{b}(z)$, depending on whether the phase is A or B. For phase A,

$$\Delta E^{c}_{a}(z) = \frac{2\pi n_a^2 A_{aa}}{d_{aa}^4}\int_z^\infty dj\int_j^\infty di\int_i^\infty \left[\frac{1}{y^5} - \frac{6}{m y^{m-1}}\right] dy \qquad (34)$$

and for phase B,

$$\Delta E^{c}_{b}(z) = \frac{2\pi n_b^2 A_{bb}}{d_{bb}^4}\int_z^\infty dj\int_j^\infty di\int_i^\infty \left[\frac{1}{y^5} - \frac{6}{m y^{m-1}}\right] dy \qquad (35)$$

In these equations A_{aa} and A_{bb} are the constants in the intermolecular potential functions for two molecules of phase A and two molecules of phase B respectively; d_{aa} and d_{bb} are the equilibrium distances of approach of two molecules of phase A and phase B respectively. $\Delta E^{c}_{a}(z)$ is the energy required to separate to infinity two bulk portions of A when the surface of each portion is at a distance z from the other. $\Delta E^{c}_{b}(z)$ is the similar quantity for phase B.

Taking the ratio of the energy of adhesion to the geometric mean of the energies of cohesion, using equations (33), (34), and (35) gives

$$\frac{\Delta E^{a}_{ab}(z)}{\left[\Delta E^{s}_{a}(z)\,\Delta E^{c}_{b}(z)\right]^{1/2}} = \frac{A_{ab}}{\left[A_{aa}A_{bb}\right]^{1/2}}\,\frac{d^{2}_{aa}\,d^{2}_{bb}}{d^{4}_{ab}} \qquad (35)$$

Note that the right hand side of (35) does not contain z so that the ratio of the energy of adhesion to the geometric mean of the energies of cohesion is independent of the distance between the two phases. Thus, z can be dropped as an argument in the left-hand side of (35). Then the equation hold for the thermodynamic energies defined by process (1).

$$\frac{\Delta E^{a}_{ab}}{\left[\Delta E^{s}_{a}\,\Delta E^{c}_{b}\right]^{1/2}} = \frac{A_{ab}}{\left[A_{aa}A_{bb}\right]^{1/2}}\,\frac{d^{2}_{aa}\,d^{2}_{bb}}{d^{4}_{ab}} \qquad (36)$$

For convenience, denote the right hand side of (36) by Φ so that

$$\frac{\Delta E^{a}_{ab}}{\left[\Delta E^{s}_{a}\,\Delta E^{c}_{b}\right]^{1/2}} = \Phi \qquad (37)$$

Although some fairly rough approximations to reality were introduced in the derivation, equation (37) is probably

not as inaccurate as these approximations would indicate. In taking ratios, some of the errors introduced by the simplifying assumptions could be expected to cancel out. This point will be discussed in detail later.

IV. The Relation between the Adhesion and Cohesion Free Energies.

By putting the expression for the force of attraction into the free energy integral and following a procedure similar to that of the last section, the free energy of adhesion of two phases can be expressed in terms of the free energy of cohesion of each phase. From (29) and (24), making use of the assumption of constant n_a and n_b,

$$\Delta F_{ab}^{a}(z) = 12\pi n_a n_b A_{ab} \int_z^\infty dx \int_x^\infty dj \int_j^\infty f\,df \int_f^\infty \left[\frac{1}{r^7} - \frac{d_{ab}^{m-6}}{r^{m+1}}\right] dr \qquad (38)$$

Again make the change of variable $y = \frac{r}{d_{ab}}$ so $r = y\,d_{ab}$ and $dr = d_{ab}\,dy$. Then

$$\Delta F_{ab}^{a}(z) = 12\pi n_a n_b A_{ab} \int_z^\infty dx \int_x^\infty dj \int_j^\infty f\,df \int_f^\infty \left[\frac{1}{d_{ab}^7 y^7} - \frac{1}{d_{ab}^7 y^{m+1}}\right] d_{ab}\,dy$$

$$\Delta F_{ab}^{a}(z) = \frac{12\pi n_a n_b A_{ab}}{d_{ab}^6} \int_z^\infty dx \int_x^\infty dj \int_j^\infty f\,df \int_f^\infty \left[\frac{1}{y^7} - \frac{1}{y^{m+1}}\right] dy \qquad (39)$$

When both phases are the same, the free energy of adhesion $\Delta F_{ab}^{a}(z)$ for two phases distant z apart, becomes the free energy of cohesion; $\Delta F_{a}^{c}(z)$ for phase A and $\Delta F_{b}^{c}(z)$ for phase B.

$$\Delta F_{a}^{c}(z) = \frac{12\pi n_a^2 A_{aa}}{d_{aa}^6}\int_z^\infty dx\int_x^\infty dj\int_j^\infty f\,df\int_f^\infty\left[\frac{1}{y^7}-\frac{1}{y^{m+1}}\right]dy \tag{40}$$

$$\Delta F_{b}^{c}(z) = \frac{12\pi n_b^2 A_{bb}}{d_{bb}^6}\int_z^\infty dx\int_x^\infty dj\int_j^\infty f\,df\int\left[\frac{1}{y^7}-\frac{1}{y^{m+1}}\right]dy \tag{41}$$

Taking the ratio of $\Delta F_{ab}^{a}(z)$ to $\left[\Delta F_{b}^{a}(z)\,\Delta F_{a}^{c}(z)\right]^{1/2}$,

$$\frac{\Delta F_{ab}^{a}(z)}{\left[\Delta F_{a}^{c}(z)\Delta F_{b}^{c}(z)\right]^{1/2}} = \frac{A_{ab}}{\left[A_{aa}A_{bb}\right]^{1/2}}\,\frac{d_{aa}^3\,d_{bb}^3}{d_{ab}^6} \tag{42}$$

Since the right hand side does not contain z, the ratio on the left is independent of the separation distance so that equation (42) holds for the free energies defined by process (1).

$$\frac{\Delta F_{ab}^{a}}{\left[\Delta F_{a}^{c}\ \Delta F_{b}^{c}\right]^{1/2}} = \frac{A_{ab}}{\left[A_{aa} A_{bb}\right]^{1/2}} \frac{d_{aa}^{3}\, d_{bb}^{3}}{d_{ab}^{6}} . \qquad (43)$$

Call the right hand side of (43) Ψ.

$$\frac{\Delta F_{ab}^{a}}{\left[\Delta F_{a}^{c}\ \Delta F_{b}^{c}\right]^{1/2}} = \Psi \qquad (44)$$

The same considerations apply to this equation as noted for equation (37)

V. Surface Energy Relations.

Equation (44) permits the evaluation of the function f of equation (20). As given in equation (4),

$$\Delta F_{ab}^{a} = \gamma_a + \gamma_b - \gamma_{ab}$$

and from equations (4') and (4''),

$$\Delta F_{a}^{c}\ \Delta F_{b}^{c} = 4\,\gamma_a\,\gamma_b$$

so that in terms of the surface and interfacial free energies (44) can be written

$$\frac{\gamma_a + \gamma_b - \gamma_{ab}}{2\sqrt{\gamma_a\,\gamma_b}} = \Psi \qquad (45)$$

Solving for γ_{ab} ,

$$\gamma_{ab} = \gamma_a + \gamma_b - 2\Psi\sqrt{\gamma_a \gamma_b} \tag{46}$$

Since Ψ is symmetrical in the phases A and B, (46) satisfies all the conditions imposed on f of equation (20).

Similarly, starting with the energies of adhesion and cohesion as given by (3), (3'), and (3''),

$$\Delta E^a_{ab} = \epsilon_a + \epsilon_b - \epsilon_{ab}$$

$$\Delta E^c_a \, \Delta E^c_b = 4\epsilon_a \epsilon_b$$

so (37) becomes,

$$\frac{\epsilon_a + \epsilon_b - \epsilon_{ab}}{2\sqrt{\epsilon_a \epsilon_b}} = \Phi \tag{47}$$

Solving for ϵ_{ab} ,

$$\epsilon_{ab} = \epsilon_a + \epsilon_b - 2\Phi\sqrt{\epsilon_a \epsilon_b} \tag{48}$$

(48) satisfies all the conditions imposed on the function g of equation (21).

The interfacial entropy S_{ab} is related to the interfacial free energy and the interfacial total energy by the thermodynamic relation

$$\gamma_{ab} = \epsilon_{ab} - TS_{ab} \tag{49}$$

From (46) and (49)

$$\epsilon_{ab} - TS_{ab} = \gamma_a + \gamma_b - 2\Psi\sqrt{\gamma_a \gamma_b} \qquad (50)$$

and substituting for ϵ_{ab} , its value from equation (48)

$$\epsilon_a + \epsilon_b - 2\Phi\sqrt{\epsilon_a \epsilon_b} - TS_{ab} = \gamma_a + \gamma_b - 2\Psi\sqrt{\gamma_a \gamma_b}$$

so

$$TS_{ab} = \epsilon_a + \epsilon_b - \gamma_a - \gamma_b - 2\Phi\sqrt{\epsilon_a \epsilon_b} + 2\Psi\sqrt{\gamma_a \gamma_b}$$

But

$$\gamma_a = \epsilon_a - TS_a$$

$$\gamma_b = \epsilon_b - TS_b$$

so

$$TS_{ab} = TS_a + TS_b - 2\Phi\sqrt{\epsilon_a \epsilon_b} + 2\Psi\sqrt{\gamma_a \gamma_b}$$

$$S_{ab} = S_a + S_b + \frac{2}{T}\left[\Psi\sqrt{\gamma_a \gamma_b} - \Phi\sqrt{\epsilon_a \epsilon_b}\right] \qquad (51)$$

VI. Summary of Derived Relations.

The main purpose of the above derivations is to lead to a method of determining the surface energy of solids so that energies of adhesion may be calculated. How this can be done by using heat of wetting data will be shown in the next section. Not all of the derived equations are necessary

for this, but all of them arise quite naturally from the theory and are useful in determining its limitations. These equations are summarized here for convenient reference.

$$\frac{\Delta E^{a}_{ab}}{\left[\Delta E^{c}_{a}\ \Delta E^{c}_{b}\right]^{1/2}} = \Phi \tag{52}$$

$$\frac{\Delta F^{a}_{ab}}{\left[\Delta F^{c}_{a}\ \Delta F^{c}_{b}\right]^{1/2}} = \Psi \tag{53}$$

$$\gamma_{ab} = \gamma_a + \gamma_b - 2\Psi\sqrt{\gamma_a \gamma_b} \tag{54}$$

$$\epsilon_{ab} = \epsilon_a + \epsilon_b - 2\Phi\sqrt{\epsilon_a \epsilon_b} \tag{55}$$

$$S_{ab} = S_a + S_b + \frac{2}{T}\left[\Psi\sqrt{\gamma_a \gamma_b} - \Phi\sqrt{\epsilon_a \epsilon_b}\right] \tag{56}$$

$$\Phi = \frac{A_{ab}}{\left[A_{aa}\ A_{bb}\right]^{1/2}} \frac{d^{2}_{aa}\ d^{2}_{bb}}{d^{4}_{ab}} \tag{57}$$

$$\Psi = \frac{A_{ab}}{\left[A_{aa}\ A_{bb}\right]^{1/2}} \frac{d^{3}_{aa}\ d^{3}_{bb}}{d^{4}_{ab}} \tag{58}$$

VII. The Surface Energy of Solids from Heats of Wetting.

When a clean, dry solid is immersed in a liquid, a solid surface of energy ϵ_s disappears and a solid-liquid interface of energy ϵ_{sL} is formed. The heat evolved is given in terms of the surface and interfacial energies by equation (6) as

$$\Delta H_w = \epsilon_{sL} - \epsilon_s \tag{59}$$

In surface thermodynamics, enthalpy and energy are considered equal since the pressure-volume term is negligible.

Writing equation (47) for a system in which one phase is solid and the other liquid,

$$\frac{\epsilon_s + \epsilon_L - \epsilon_{sL}}{2\sqrt{\epsilon_s \epsilon_L}} = \Phi \tag{60}$$

Making use of (59) gives,

$$\frac{\epsilon_L - \Delta H_w}{2\sqrt{\epsilon_s \epsilon_L}} = \Phi \tag{61}$$

and solving for ϵ_s,

$$\epsilon_s = \frac{(\epsilon_L - \Delta H_w)^2}{4\epsilon_L \Phi^2} \tag{62}$$

ΔH_w and ϵ_L are measurable quantities, so provided that Φ can be evaluated, (62) can be used to compute the surface energy of solids.

VIII. The Surface Free Energy of Solids and the Free Energy of Adhesion.

When phase A is a solid and phase B a liquid, equation (45) becomes

$$\frac{\gamma_S + \gamma_L - \gamma_{SL}}{2\sqrt{\gamma_S \gamma_L}} = \Psi \qquad (63)$$

But since $\gamma_S + \gamma_L - \gamma_{SL} = \Delta F_{SL}^a$, the free energy of adhesion of the solid to the liquid,

$$\frac{\Delta F_{SL}^a}{2\sqrt{\gamma_S \gamma_S}} = \Psi \qquad (64)$$

Solving for γ_S,

$$\gamma_S = \frac{\left(\Delta F_{SL}^a\right)^2}{4\gamma_L \Psi^2} \qquad (65)$$

The free energy of adhesion ΔF_{SL}^a is a measurable quantity as shown by equations (9) to (12) so that γ_S can be computed from (65) if Ψ is known.

IX. Contact Angles and Surface Tension.

Young's equation gives the angle of contact of a liquid with a solid in terms of the surface tensions as[9]

$$\gamma_{SL} + \gamma_L \cos\theta = \gamma_{SV} \tag{66}$$

θ = contact angle

γ_{SL} = free energy of the solid-liquid interface

γ_L = surface free energy of the liquid

γ_{SV} = surface free energy of the solid in contact with the vapor of the liquid.

The difference ($\gamma_S - \gamma_{SV}$) is the equilibrium film pressure π_e , i.e.

$$\pi_e \equiv \gamma_S - \gamma_{SV} \tag{67}$$

so equation (66) can be expressed in terms of γ_S as

$$\gamma_{SL} + \gamma_L \cos\theta = \gamma_S - \pi_e \tag{68}$$

Applying equation (63) to (68) gives

$$\gamma_L (1 + \cos\theta) + \pi_e = 2\bar{\Psi}\sqrt{\gamma_S \gamma_L} \tag{69}$$

This equation shows how the contact angle depends on the surface free energies of the solid and liquid phases. Solving for γ_S ,

$$\gamma_S = \frac{\left[\gamma_L (1 + \cos\theta) + \pi_e\right]^2}{4\bar{\Psi}^2 \gamma_L} \tag{70}$$

Cos θ is restricted to the range of values between -1 and +1. Putting these extreme values for cos θ into (70) shows that in order for a liquid solid system to exhibit a contact angle between 0^{o} and 180^{o}, the following inequality must hold.

$$\frac{\pi_e^2}{4\Psi^2\gamma_L} < \gamma_S < \frac{(2\gamma_L + \pi_e)^2}{4\Psi^2\gamma_L} \qquad (71)$$

The inequality (71) is consistent with the fact that low surface energy liquids, such as hydrocarbons, on high surface energy solids, such as metal oxides, show no contact angle; whereas high energy liquids, such as water, on low energy solids, such as paraffin, have contact angles greater than zero.

X. The Distribution of Energy over a Solid Surface.

The fact that the energy varies from point to point on a surface has been pointed out by a number of investigators[10,11,12], but no satisfactory method has been given in the literature for the direct experimental determination of the distribution function for the surface energy of solids. The following development presents a method for measuring the distribution function in terms of the fraction of the surface having energy greater than some specified amount. The experimental basis of the method is the deter-

mination of the heat of wetting as a function of the amount of preadsorbed material on the solid surface.

Let θ = the fraction of the surface that has energy greater than ϵ_s .

$\bar{\epsilon}_s$ = the average energy of that part of the surface having energy less than .

In general, ϵ_s will decrease with increasing θ and a graphic representation of the variation of ϵ_s with θ will have the form of Figure II

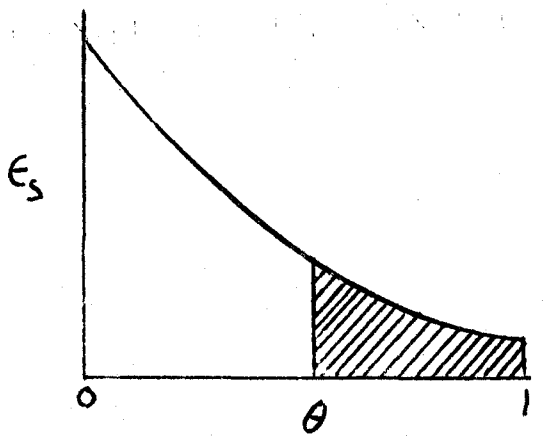

Figure II

$\bar{\epsilon}_s$ is the average energy of the shaded portion in Figure II and is given by

$$\bar{\epsilon}_s = \frac{1}{1-\theta}\int_{\theta}^{1} \epsilon_s \, d\theta \qquad (72)$$

Differentiating under the integral sign and solving for ϵ_s,

$$\epsilon_s = \bar{\epsilon}_s - (1-\theta)\frac{d\bar{\epsilon}_s}{d\theta} \qquad (73)$$

Equation (73) is a relationship between the actual energy ϵ_s at some point on the surface, and the average energy of all parts of the surface having energy less than ϵ_s. It can be used to calculate ϵ_s as a function of θ if a measure of $\bar{\epsilon}_s$ can be obtained.

Assume that a fraction θ of a solid surface is covered with some material such as stearic or perfluorodecanoic acid. Then, if the organic acid is preferentially adsorbed at high energy sites, this θ is identical with the θ in the previous equations. Let ΔH_w be the heat of wetting per cm.^{2} of surface, θ of which is covered with some preadsorbed material. Also, let

h_m = heat of wetting per cm.^{2} of that part of the surface which is covered with the preadsorbed film. This value is constant, for a given film-forming substance, with varying coverage if the preadsorbed molecules are large enough to "lag out" surface heterogeneity.

$\bar{h}$ = average heat of wetting of the bare part of the surface.

The total heat of wetting ΔH_w is the sum of the heats of wetting of the bare part and of the covered part of the surface according to the equation

$$\Delta H_w = (1-\theta)\bar{h} + \theta h_m \qquad (74)$$

Solving for $\bar{h}$,

$$\bar{h} = \frac{1}{1-\theta}\left[\Delta H_w - \theta h_m\right] \tag{75}$$

In effect, preadsorption blocks out the upper range of energies. The contribution of the bare part of the surface to the heat of wetting is given by (75), and this gives information about the variation of the energy with coverage.

The average heat of wetting for the bare part of the surface is also given by

$$\bar{h} = \bar{\epsilon}_s - \bar{\epsilon}_{sl} \tag{76}$$

where $\bar{\epsilon}_{sl}$ is the average energy of the solid-liquid interface for that fraction of the surface having energy less than ϵ_s . Now all that is needed to apply (73) is an independent relation between $\bar{\epsilon}_{sl}$ and $\bar{\epsilon}_s$. This relation has already been given by equation (62). Applied to the average energy of the bare part of the surface, (62) is

$$\bar{\epsilon}_s = \frac{\left(-\bar{h} + \epsilon_l\right)^2}{4\epsilon_l \Phi^2} \tag{77}$$

Differentiating,

$$\frac{d\bar{\epsilon}_s}{d\theta} = -\frac{(\epsilon_l - \bar{h})}{2\epsilon_l \Phi^2}\frac{d\bar{h}}{d\theta} \tag{78}$$

Putting (77) and (78) into (73)

$$\epsilon_s = \frac{(-\bar{h} + \epsilon_L)^2}{4\epsilon_L \Phi^2} + (1-\theta)\frac{(\epsilon_L - \bar{h})}{2\epsilon_L \Phi^2}\frac{d\bar{h}}{d\theta} \qquad (79)$$

or

$$\epsilon_s = \frac{(\epsilon_L - \bar{h})}{4\epsilon_L \Phi^2}\left[\frac{1}{2}(\epsilon_L - \bar{h}) + (1-\theta)\frac{d\bar{h}}{d\theta}\right] \qquad (80)$$

Even if Φ were completely unknown, equation (80) would make possible the calculation of ϵ_s as a function of θ, (i.e. the surface energy distribution function) within a constant factor since Φ is a constant for a given system.

XI. The Evaluation of Φ and Ψ.

From its definition above, Φ is given

$$\Phi = \frac{A_{ab}}{[A_{aa} A_{bb}]^{1/2}} \frac{d_{aa}^2 d_{bb}^2}{d_{ab}^4} \qquad (81)$$

To evaluate Φ exactly, not only the equilibrium distance between molecules, but also the constants in the potential energy functions must be known. Since this method of calculation can be applied to only the simplest of systems, an alternate procedure will be adopted here.

First, it is assumed that the equilibrium distance of approach can be taken as proportional to the cube root of the molar volume:

$$d_{aa} = C V_a^{1/3} \tag{82}$$

$$d_{bb} = C V_b^{1/3} \tag{83}$$

V_a = molar volume of phase A.

V_b = molar volume of phase B.

C = proportionality constant.

Taking the distance of closest approach of a molecule of A to a molecule of B as the arithmetic mean of the distance of closest approach of the like molecules,

$$d_{ab} = \frac{1}{2}\left(d_{aa} + d_{bb}\right) \tag{84}$$

Equations (82), (83), and (84) give

$$d_{ab} = \frac{C}{2}\left(V_a^{1/3} + V_b^{1/3}\right) \tag{85}$$

Substituting (82), (83), and (85) into (81) gives as

$$\Phi = \frac{A_{ab}}{\left[A_{aa} A_{bb}\right]^{1/2}} \frac{16 V_a^{2/3} V_b^{2/3}}{\left[V_a^{1/3} + V_b^{1/3}\right]^4} \tag{86}$$

Strictly, equations (82) through (85) are valid only for spherical molecules, but if the molecules of both phases are of similar geometry, the ratio term of the molar volumes is sufficiently accurate for computing Φ.

To simplify (86) even further, make the additional assumption that

$$A_{ab} = \left(A_{aa}\, A_{bb}\right)^{1/2} \tag{87}$$

This assumption is not completely unwarranted, and is in fact very nearly true for molecules that have similar types of potential functions[13]. Using (87), equation (86) becomes

$$\Phi = \frac{16\, V_a^{2/3} V_b^{2/3}}{\left(V_a^{1/3} + V_b^{1/3}\right)^4} \tag{88}$$

If the value of Φ given by (88) is used, the theory is strictly valid only for systems whose two phases are sufficiently alike in two respects. First, their molecular force fields must be similar enough to make (87) at least approximately true. Second, the molecular geometry must be similar enough so that the ratio term involving equilibrium distances can be replaced by the ratio term involving molar volumes.

Ψ is defined by

$$\Psi = \frac{A_{ab}}{(A_{aa} A_{bb})^{1/2}} \qquad (89)$$

An exactly similar argument is employed to express Ψ in terms of molar volumes as was used in obtaining equation (88). The only difference is in the power of the d's, so that the result is

$$\Psi = \frac{64 V_a V_b}{(V_a^{1/3} + V_b^{1/3})^6} \qquad (90)$$

The same limitations apply to equation (90) as to equation (88).

The mathematical form of Φ and Ψ is such that they are in general of the order of magnitude of unity; and in a large number of cases, the deviation from unity is small. If both phases are identical, $d_{aa} = d_{bb} = d_{ab}$ and $A_{aa} = A_{bb} = A_{ab}$ so that Φ and Ψ are both exactly equal to one. The rule can be given that the more alike the two phases, the closer Φ and Ψ approach unity.

As a simplification in calculating the surface energy of solids from heat of wetting data by equation (62), and the surface free energy from work of adhesion by equation (65), Φ and Ψ can be taken equal to unity, provided that the wetting liquid is relatively similar to the solid in

molecular size and in polarity. This means that for a non-polar solid such as graphite, the wetting data of a liquid such as benzene should be used; while for polar solids such as metallic oxides, polar liquids such as water should be used. Indeed, it will be shown that the equations hold when a hydroxyl containing polar compound is used with polar solids. This is interpreted in terms of molecular orientation at the interface. This orientation presents a hydroxyl containing layer to the solid which is very similar to the solid itself.

The approximation introduced by calling Φ and Ψ equal to one when like phases are considered is no greater than the other approximations of the theory. Besides, it greatly simplifies matters since the necessity of deciding on the values for the A's and the d's is avoided. The range of validity of the equations in this form will be investigated in a later section.

THEORETICAL DEVELOPMENT. II. DISCUSSION AND LIMITATIONS

I. The Validity of the Fowler-Guggenheim Integrals.

The integrals (22), (23), and (24) form the basis on which the rest of the theory is built, and it is important to examine the approximations that went into them, and the extent to which they affect the final formula.

As is evident from the derivation, the two phases are treated as if they consisted of a rigid three dimensional array of point centers of force; the distribution of these centers in space being described by the functions n_a and n_b. In other words, the equations compute the molecular attractions only when each molecule is in an average position of minimum potential energy. The effect of thermal motion is neglected. It is difficult to estimate the inaccuracy introduced by this treatment, but it is probably no greater than that due to the subsequent assumptions. Since the same type of error would be expected in the adhesion and cohesion integrals, a considerable part of this error would cancel on taking the ratios indicated by equations (37) and (44).

The second important idealization in the Fowler-Guggenheim integrals is the complete planarity and homogeneity of the surfaces and interfaces involved. As long as the adhesive system consists of two liquid phases this introduces no error; but if one of the phases is solid, there is

considerable departure from a plane, homogeneous interface. In the case of a powdered solid immersed in a liquid for example, the solid-liquid interface is jagged and heterogeneous. Thus, the energy of adhesion will be greater than if the interface were completely planar. The following diagram illustrates how corners and edges contribute more than planes to the adhesion energy.

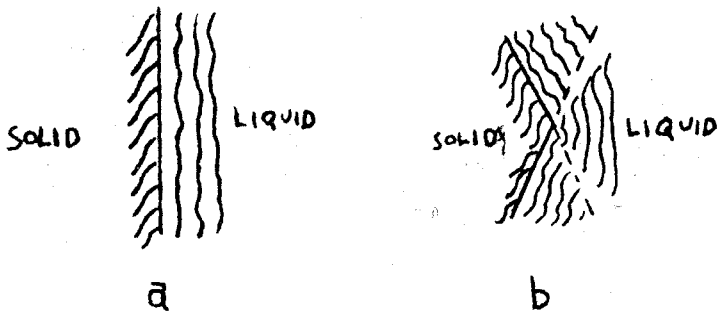

Figure III

Figure IIIa represents a plane solid-liquid interface and Figure IIIb represents a jagged solid-liquid interface of the same area. The figure shows that the jagged solid surface interacts with a greater amount of liquid than the plane solid surface. The excess of liquid contributing to the adhesion energy is that between the dotted lines.

If the solid surface is not too heterogeneous and the corners not too sharp, the adhesion energy will not be greatly different from that for a plane interface. This is because the interaction energy between molecules dies out rapidly with distance, and only the few molecules in the

corner of the angle formed by the dotted lines add appreciable amounts of energy to the adhesive system.

This error is only partially corrected for in taking ratios of adhesion to cohesion energies because the cohesional energy of a liquid is defined in terms of surface energy referred to a plane surface. Cohesive failure of the solid, however, may be defined in such a way as to produce the solid surface taking part in the interface, so that the same kind of error occurs in the energy of cohesion for the solid as in the energy of adhesion. This situation tends to bring the error in the ratios down to the square root of its value in the adhesion integrals.

II. The Assumption of Spherical Molecules.

The assumption of spherical molecules was used in two places: first, in choosing the potential $\mathcal{E}_{ab}$ as a function of distance it was assumed that the potential field was spherically symmetrical about the molecule so that only the radial distance parameter appeared in the equation. Second, in evaluating Φ and Ψ, the equilibrium distances were related to the molar volumes in a way that can be strictly true only for spheres. The particles in solids such as graphite or metallic oxides can generally be taken as spherical. At ordinary temperatures liquids usually possess enough rotational motion to make the sphericity approximation

fairly accurate[14] unless the molecules are extremely polar or asymmetric as in the case of long chain fatty acids. If the molecules of the two phases are geometrically very dissimilar, the constants C in equations (82) and (83) are not the same and equation (84) does not necessarily hold. At any rate the equations can be applied to systems of any molecular geometry with the expectation that, all other factors being equal, they will give best results with systems whose molecules are spherical. Systems whose two phases have molecules that are not spherical and have greatly different molecular geometries would be expected to give the greatest discordance between calculated and experimental values. If the two phases have molecules that are not spherical but are similar, an error intermediate to that of the previous two cases would be introduced. Later, it will be seen that molecular geometry is sometimes completely overshadowed by other factors.

III. The Assumption of Constant Microscopic Densities.

The microscopic densities n_a and n_b in the integrals of Fowler and Guggenheim are not constants, but depend on the distance parameters. In general, n_a is a function of r, f, and j, and n_b is a function of j. For liquid phases, since there is only short-range order, n_a may be taken to be the radial distribution functions for the phase A, and n_b the

density distribution function of phase B.

Probably the greater part of the error in assuming n_a and n_b to be constants arises from the fact that molecules at surfaces and interfaces are in a different condition than those in the bulk phase. The distances between molecules in surfaces and interfaces is less than in the bulk phase so the values of n_a and n_b increase rather abruptly at phase boundaries. Since the molecular interaction energy dies off so rapidly with distance, the molecules at the interface contribute the most to the adhesion energy, and the difference in density affects the adhesion integral to a greater extent than if it occurred in the bulk phase at some distance from the interface.

If the molecules are asymmetric, orientation may occur at the interface when one of the phases is liquid. Evidence for such orientation is well known[15,16]. In the case of adhesion between a long chain alcohol or fatty acid and some polar phase such as water or metallic oxides, the carboxyl or hydroxyl group is directed toward the interface, and most of the adhesion energy is due to interaction between polar-polar groups. Use will be made of this situation later in obtaining the surface energy of solids from heat of wetting data.

IV. The Nature of the Intermolecular Potential Function.

It has been fairly well established that many simple molecules attract each other according to the inverse sixth power rule[17]. The form of the repulsive term is somewhat more doubtful, but the function $B_{ab}r^{-m}$ seems a reasonable approximation where m is somewhere between 8 and 12. As the derivation shows, the exact value of m is immaterial in this work.

If the ratio $A_{ab}/(A_{aa}A_{bb})^{1/2}$ is not unity, the values of Φ and Ψ given above are, of course, in error and a consideration of the possible deviation of this ratio from unity is necessary.

The constant A_{ab} is given by[18]

$$A_{ab} = \frac{2\mu_a^2\mu_b^2}{3kT} + \left(\mu_a^2\alpha_b + \mu_b^2\alpha_a\right) + \frac{3}{4}h\alpha_a\alpha_b\frac{\nu_a\nu_b}{\nu_a+\nu_b} \qquad (91)$$

where μ_a is the dipole moment of a molecule of phase A,

α_a is the polarizability of a molecule of phase A

ν_a is the natural frequency of oscillation of a molecule of phase A

μ_b, α_b and ν_b are the corresponding quantities for a molecule of phase B

k is Boltzmann's constant, and

T the absolute temperature

h is Planck's constant

Similarly A_{aa} and A_{bb} are

$$A_{aa} = \frac{2\mu_a^4}{3kT} + 2\mu_a^2\alpha_a + \frac{3}{4}h\alpha_a^2\frac{\nu_a}{2} \tag{92}$$

$$A_{bb} = \frac{2\mu_b^4}{3kT} + 2\mu_b^2\alpha_b + \frac{3}{4}h\alpha_b^2\frac{\nu_b}{2} \tag{93}$$

The first term in these equations arises from the dipole-dipole interaction between molecules, the second term from the dipole-induced dipole interactions, and the third term from dispersion interactions.

If $\mu_a = \mu_b = 0$ so that only dispersion forces are operative between the molecules, (91), (92), and (93) give

$$\frac{A_{ab}}{(A_{aa}A_{bb})^{1/2}} = \frac{(\nu_a\nu_b)^{1/2}}{\frac{1}{2}(\nu_a+\nu_b)} \tag{94}$$

The right hand side of (94) is the ratio of a geometric to an arithmetic mean. Since ν_a and ν_b are generally of the same order of magnitude the ratio may be taken as unity with an error that is certainly less than the other errors introduced in the derivations.

In general

$$\frac{A_{ab}}{(A_{aa}A_{bb})^{1/2}} = \frac{\frac{2\mu_a^2\mu_b^2}{3kT} + (\mu_a^2\alpha_b + \mu_b^2\alpha_a) + \frac{3}{4}h\alpha_a\alpha_b\frac{\nu_a\nu_b}{\nu_a+\nu_b}}{\left(\frac{2}{3}\frac{\mu_a^4}{kT} + 2\mu_a^2\alpha_a + \frac{3}{4}h\alpha_a^2\frac{\nu_a}{2}\right)^{1/2}\left(\frac{2}{3}\frac{\mu_b^4}{kT} + 2\mu_b^2\alpha_b + \frac{3}{4}h\alpha_b^2\frac{\nu_b}{2}\right)^{1/2}} \quad (95)$$

If the dispersion forces are small compared to the dipole forces, the terms containing ν_a and ν_b can be neglected and

$$\frac{A_{ab}}{(A_{aa}A_{bb})^{1/2}} = \frac{\frac{2\mu_a^2\mu_b^2}{3kT} + (\mu_a^2\alpha_b + \mu_b^2\alpha_a)}{\left(\frac{2}{3}\frac{\mu_a^4}{kT} + 2\mu_a^2\alpha_a\right)^{1/2}\left(\frac{2}{3}\frac{\mu_b^4}{kT} + 2\mu_b^2\alpha_b\right)^{1/2}} \quad (96)$$

Forthermore, if $\mu_a = \mu_b$,

$$\frac{A_{ab}}{(A_{aa}A_{bb})^{1/2}} = \frac{\frac{2\mu_a^4}{3kT} + \mu_a^2(\alpha_a+\alpha_b)}{\left(\frac{2}{3}\frac{\mu_a^4}{kT} + 2\mu_a^2\alpha_a\right)^{1/2}\left(\frac{2}{3}\frac{\mu_a^4}{kT} + 2\mu_a^2\alpha_b\right)^{1/2}} \quad (97)$$

If in addition $\alpha_a = \alpha_b$, the ratio $A_{ab}/(A_{aa}A_{bb})^{1/2}$ becomes unity. Even if α_a and α_b are somewhat different, this ratio will not deviate too much from unity.

From these considerations, the following statements can be made:

1. For adhesive systems, $A_{ab}/(A_{aa}A_{bb})^{1/2} \approx 1$ when:
   a. Both phases are non-polar

b. Both phases are polar, the dipole moments of molecules of both types are the same, and the polarizability of both types of molecules are the same.

b. Slight deviations from the above conditions will not seriously alter the value of the ratio.

For best results therefore, the derived equations should be applied to systems composed of phases that are similar in polarity and polarizability. It will be shown later that when the two phases differ widely in polarity, the deviation of the calculated from experimental values is greater than when the two phases are of similar polarity. Fortunately, in computing the surface energy of solids by equation (62) it is in general possible to choose heat of wetting data for polar liquids on polar solids and non-polar liquids on non-polar solids.

V. The Cancellation of Errors in the Energy Ratios.

Because the same assumptions were applied to the adhesion and cohesion integrals, the errors in the numerator and denominator of the ratios of equations (52) and (53) can be expected to be of roughly the same magnitude. Consequently, part of the errors will cancel in the ratios, and the equations should be better than the assumptions indicate. The energy ratio is given by

$$\Phi = \frac{\Delta E^{d}_{ab}}{\left(\Delta E^{c}_{a}\ \Delta E^{c}_{b}\right)^{1/2}} \tag{98}$$

The error in Φ is approximated by the total differential $d\Phi$

$$d\Phi = \frac{\partial \Phi}{\partial(\Delta E^{a}_{ab})} d(\Delta E^{a}_{ab}) + \frac{\partial \Phi}{\partial(\Delta E^{c}_{a})} d(\Delta E^{c}_{a}) + \frac{\partial \Phi}{\partial(\Delta E^{c}_{b})} d(\Delta E^{c}_{b}) \tag{99}$$

The relative error is

$$\frac{d\Phi}{\Phi} = \frac{\partial \Phi}{\partial(\Delta E^{d}_{ab})} \frac{d(\Delta E^{d}_{ab})}{\Phi} + \frac{\partial \Phi}{\partial(\Delta E^{c}_{a})} \frac{d(\Delta E^{c}_{a})}{\Phi} + \frac{\partial \Phi}{\partial(\Delta E^{c}_{b})} \frac{d(\Delta E^{c}_{b})}{\Phi} \tag{100}$$

or

$$\frac{d\Phi}{\Phi} = \frac{\partial \ln \Phi}{\partial(\Delta E^{d}_{ab})} d(\Delta E^{d}_{ab}) + \frac{\partial \ln \Phi}{\partial(\Delta E^{c}_{a})} d(\Delta E^{c}_{a}) + \frac{\partial \ln \Phi}{\partial(\Delta E^{c}_{b})} d(\Delta E^{c}_{b}) \tag{101}$$

Taking logarithms of (98)

$$\ln \Phi = \ln(\Delta E^{d}_{ab}) - \frac{1}{2} \ln(\Delta E^{c}_{a}) - \frac{1}{2} \ln(\Delta E^{c}_{b}) \tag{102}$$

from which

$$\frac{\partial \ln \Phi}{\partial(\Delta E^a_{ab})} = \frac{1}{\Delta E^a_{ab}} \;, \quad \frac{\partial \ln \Phi}{\partial(\Delta E^c_a)} = \frac{1}{\Delta E^c_a} \;, \quad \frac{\partial \ln \Phi}{\partial(\Delta E^c_b)} = \frac{1}{\Delta E^c_b}$$

Therefore

$$\frac{d\Phi}{\Phi} = \frac{d(\Delta E^a_{ab})}{\Delta E^a_{ab}} - \frac{1}{2}\left[\frac{d(\Delta E^c_a)}{\Delta E^c_a} + \frac{d(\Delta E^c_b)}{\Delta E^c_b}\right] \qquad (103)$$

Equation (103) shows that the percentage error in the ratio Φ is equal to the percentage error in the adhesion integral minus one-half the sum of the percentage errors of the cohesion integrals. Thus, no matter how large the errors in the integrals, the error in the ratio will be small provided the adhesion and cohesion errors are very similar.

Just how the error in the adhesion integral must be related to the errors in the cohesion integrals for a given accuracy in the ratios can be determined from (103). If an accuracy in Φ of plus or minus $(100\ x)\%$ is desired, then (103) imposes the condition

$$\frac{d(\Delta E^a_{ab})}{\Delta E^a_{ab}} = \frac{1}{2}\left(\frac{d(\Delta E^c_a)}{\Delta E^c_a} + \frac{d(\Delta E^c_b)}{\Delta E^c_b}\right) \pm \chi \qquad (104)$$

This result indicates that considerable latitude is permitted in the error of the adhesion integral, for a

given error in the cohesion integrals. For example, if $x = 0.05$, and the cohesion integrals are each 10% in error,

$$\frac{d(\Delta E^a_{ab})}{\Delta E^a_{ab}} = \frac{1}{2}(0.2) \pm 0.05) = 0.1 \pm 0.05$$

so the error in the adhesion integral can vary anywhere from 5 to 15% and still not make the error in $\bar{\Phi}$ greater than 5%. Of course, the closer $\frac{d(\Delta E^a_{ab})}{\Delta E^a_{ab}}$ is to 0.1, the less the error in $\bar{\Phi}$. If a larger error in $\bar{\Phi}$ is permitted, a correspondingly larger range is permitted to the adhesion error. If $x = 0.1$ so that an error of $\pm$ 10% is tolerated, and if the cohesion integrals are in error by 20%,

$$\frac{d(\Delta E^a_{ab})}{\Delta E^a_{ab}} = \frac{1}{2}(0.4) \pm 0.1 = 0.2 \pm 0.1$$

so the adhesion integral may be in error anywhere from 10 to 30% and still keep the error in $\bar{\Phi}$ within 10%.

The conclusion to be drawn from the preceding discussion is that the theory should give better results the more alike the two phases of the adhesive system are with respect to their polarity, molecular geometry, density, and type of intermolecular potential functions. The explanation of serious deviations from the equations is to be looked for in wide differences between the two phases in one of these particulars.

These limitations apply of course only to equations in which Φ or $\bar{\Psi}$ appear. As will be shown below, the adhesion energy, which is the most important quantity in this work, can be obtained exactly in the case of ice-solid systems.

THEORETICAL DEVELOPMENT. III. APPLICATION TO ICE ADHESION

I. The Surface Energy of Ice from Adsorption Data.

According to equation (14) the energy of adhesion is related to the energy of adsorption by

$$\Delta E^{a}_{ab} = \frac{(Q_a - Q_s)}{\Sigma} + 2\epsilon_a \qquad (14)$$

Applying this equation to the adsorption of water vapor on solids below 0° C., i.e. the case of ice-solid adhesion, and calling the net heat of adsorption per cm.^{2} H_a

$$\Delta E^{a}_{Is} = H_a + 2\epsilon_I \qquad (105)$$

ΔE^{a}_{Is} = adhesion energy of ice to the other solid

H_a = net integral heat of adsorption of ice on the solid per cm.^{2} of surface

ϵ_I = the surface energy of ice.

From equation (52)

$$\Delta E^{a}_{Is} = \Phi_1 (\Delta E^{c}_{I} \Delta E^{c}_{s})^{1/2} \qquad (106)$$

ΔE^{c}_{I} = energy of cohesion of ice

ΔE^{c}_{s} = energy of cohesion of the solid

Φ_1 refers to the ice-solid system.

The energy of cohesion is just half the surface energy

$$\Delta E_I^c = 2\epsilon_I$$

$$\Delta E_s^c = 2\epsilon_s$$

so

$$\Delta E_{Is}^a = 2\Phi_1\sqrt{\epsilon_I \epsilon_s} \tag{107}$$

From (105)

$$H_a + 2\epsilon_I = 2\Phi_1\sqrt{\epsilon_I \epsilon_s} \tag{108}$$

Solving for

$$\epsilon_I = \frac{1}{2}\left[\left(\Phi_1^2\epsilon_s - H_a\right) \pm \sqrt{\left(H_a - \Phi_1^2\epsilon_s\right)^2 - H_a^2}\right] \tag{109}$$

But from equation (62) ϵ_s is given by

$$\epsilon_s = \frac{\left(\epsilon_L - \Delta H_w\right)^2}{4\epsilon_L \Phi_2^2} \tag{110}$$

Here, Φ_2 refers to the water-solid system.

The ratio of Φ_1, to Φ_2 can be obtained by applying equation (81). It is

$$\frac{\Phi_1}{\Phi_2} = \frac{d_{II}^2 d_{ss}^2}{d_{Is}^4} \frac{d_{ws}^4}{d_{ww}^2 d_{ss}^2} = \frac{d_{II}^2}{d_{ww}^2} \frac{d_{ws}^4}{d_{Is}^4} \qquad (111)$$

or, in terms of molar volumes from equation (86)

$$\frac{\Phi_1}{\Phi_2} = \frac{V_I^{2/3}}{V_w^{2/3}} \frac{\left(V_w^{1/3} + V_s^{1/3}\right)^4}{\left(V_I^{1/3} + V_s^{1/3}\right)^4} \qquad (112)$$

d_{II} = intermolecular distance between ice molecules

d_{ww} = intermolecular distance between water molecules

d_{ss} = intermolecular distance between molecules of the solid

d_{Is} = intermolecular distance between molecule of ice and molecule of solid

d_{ws} = intermolecular distance between water molecule and molecule of the solid

V_I = molar volume of ice

V_w V_w = molar volume of water

V_s = molar volume of the solid

These ratios are quite insensitive to moderate changes in the d's or V's and a difference between V_I and V_w of about 10% would affect the value of Φ only slightly. Furthermore, the first few layers of water molecules on the solid surface are strongly influenced by the surface forces,

and their structure is largely independent of the structure of the bulk phase. Thus the intermolecular distances for these first layers is the same regardless of the state of the bulk phase. Since most of the adhesion energy is due to these first layers, it is really incorrect to use V_w and V_i separately in the above equations. Rather some molar volume term should be used that refers to the molecules in the surface phase. This molar volume term would be the same whether the bulk phase be water or ice. Thus the ratio Φ_1/Φ_2 can be taken as unity to an excellent degree of approximation, i.e.

$$\frac{\Phi_1}{\Phi_2} = 1 \tag{113}$$

Keeping this in mind, putting (110) into (109) gives

$$\epsilon_I = \frac{1}{2}\left[\frac{(\epsilon_L - \Delta H_w)^2}{4\epsilon_L} - H_a + \sqrt{\left[H_a - \frac{(\epsilon_L - \Delta H_w)^2}{4\epsilon_L}\right]^2 - H_a^2}\right] \tag{114}$$

So the surface energy of ice can be computed.

There is no difficulty in choosing between the plus and minus sign of the quadratic solution. The minus sign gives a surface energy value that is far below that of water, so the positive sign is chosen.

II. The Energy of Adhesion of Ice to Solids.

The value of ϵ_I calculated from experiments using the theory described above, is practically independent of the approximations of the theory. Hence it is possible to compute a value for the adhesion energy of ice to solids that is also independent of the theory. From (107) and (110), using (113)

$$\Delta E^a_{Is} = (\epsilon_L - \Delta H_w)\sqrt{\frac{\epsilon_I}{\epsilon_L}} \qquad (115)$$

ϵ_I is known from (114) so ΔE^a_{Is} can be calculated. In these equations ϵ_L must be the surface energy of water and ΔH_w the heat of wetting of the solid with water.

TEST OF THE THEORY USING LITERATURE DATA

I. Liquid-Liquid Systems

To show that the theory leads to reasonable equations, a brief comparison of theory with literature data will be given for liquid-liquid systems. Equations (52) through (55), using the values of Φ and Ψ given by (88) and (90), contain quantities that are all measurable if both phases are liquid. This provides a direct check on the theory. Tables I and II compare the experimental and theoretical values for the energy ratios. Tables III and IV compare the experimental and theoretical values for the interfacial tension and the interfacial energy respectively.

The results in Table I indicate that the theoretical energy ratio can be in considerable error for polar-nonpolar systems. In the cases cited the deviations range from 10 to 36%. Assuming $\Phi = 1$ for heptylic acid, n-octanol and sec.-octanol gives reasonable results, the deviation ranging from 6 to 10%. For such polar-polar systems, orientation is expected and the orienting group is about the same size as the water molecule.

Table II shows that the theory works much better for the free energy ratio than for the energy ratio. Although the deviation for water-nonpolar systems is still in the range of 20 to 30%, the deviation for water-polar

Table I

Test of equation (52), $\frac{\Delta E^a_{ab}}{(\Delta E^c_a \Delta E^c_b)^{1/2}} = \Phi$, at 20° C.

System		ΔE^a_{ab}	ΔE^c_a	ΔE^c_b	Φ_{ex}	Φ_{ca}	Φ'_{ca}	% Deviation	
Phase A	Phase B							Φ_{ca}	$\Phi_{ca'}$
Water	n-Heptane	92.8	236	99.8	0.602	0.788	---	31	--
Water	n-Tetradecane	97.7	236	105.2	0.620	0.682	---	10	--
Water	Benzene	134	236	138.0	0.742	0.875	---	18	--
Water	Ethylene bromide	126.4	236	156.4	0.654	0.888	---	36	--
Water	Heptylic acid	150.5	236	105.2	0.954	0.784	1.0	18	6
Water	n-Octanol	164.6	236	101.0	1.07	0.780	1.0	27	7
Water	sec-Octanol	170.1	236	100.8	1.10	0.780	1.0	29	10

All energy values are given in ergs/cm.^{2}

The energy data is taken from reference 19.

$$\Phi_{ex} = \frac{\Delta E^a_{ab}}{(\Delta E^c_a \Delta E^c_b)^{1/2}} \quad , \quad \Phi_{ca} = \frac{16 V_a^{2/3} V_b^{2/3}}{(V_a^{1/3} + V_b^{1/3})^4} \quad , \quad \Phi'_{ca} = 1$$

The molar volume data is taken from references 20 and 21.

Table II

Test of equation (53), $\frac{\Delta F^a_{ab}}{(\Delta F^c_a \Delta F^c_b)^{1/2}} = \Psi$, at 25° C.

System		ΔF^a_{ab}	ΔF^c_a	ΔF^c_b	Ψ_{ex}	$^a\Psi_{ca}$	$^b\Psi'_{ca}$	% Deviation*	
Phase A	Phase B							a	b
Water	Carbon tetrachloride	55.8	145.6	53.4	0.635	0.790	---	24.8	-
Water	Benzene	67.6	145.6	57.8	0.738	0.820	---	11.1	-
Water	Heptane	43.0	145.6	40.8	0.559	0.700	---	26.2	-
Water	Bromobenzene	69.9	145.6	70.4	0.692	0.703	---	15.9	-
Water	Ethyl bromide	65.7	145.6	48.4	0.793	0.840	---	1.6	-
Water	Nitrobenzene	90.6	145.6	86.0	0.809	0.775	---	4.2	-
Water	Methylene iodide	75.1	145.6	101.6	0.618	0.830	---	34.3	-
Water	Heptylic acid	93.4	145.6	56.2	1.03	0.686	1.0	33	3
Water	n-Octanol	91.8	145.6	55.0	1.02	0.690	1.0	32.4	2
Water	sec-Octanol	89.9	145.6	52.6	1.03	0.690	1.0	32.4	3
Water	Caprylic acid		145.6		1.03	---	1.0	-	3

$$\Psi_{ex} = \frac{\Delta F^a_{ab}}{(\Delta F^c_a \Delta F^c_b)^{1/2}} \quad , \quad \Psi_{ca} = \frac{64\, V_a V_b}{(V_a^{1/3} + V_b^{1/3})^6} \quad , \quad \Psi'_{ca} = 1$$

Energy data taken from references 19 and 22.

* Deviations under "a" were computed using Ψ_{ca} under "a" and deviations under "b" were computed using Ψ'_{ca} under "b".

Table III

Test of equation (54), $\gamma_{ab} = \gamma_a + \gamma_b - 2\Psi\sqrt{\gamma_a\gamma_b}$ at 20° C.

System							
Phase A	Phase B	γ_a	γ_b	Ψ	γ_{ab} Expt.	γ_{ab} Calc.	% Deviation
Water	Carbon tetrachloride	72.8	26.7	0.790	43.7	29.0	33.6
Water	Benzene	72.8	28.9	0.820	34.1	26.4	22.8
Water	Heptane	72.8	20.4	0.700	50.2	39.2	21.9
Water	Bromobenzene	72.8	35.2	0.703	38.1	26.4	30.7
Water	Ethyl bromide	72.8	24.2	0.840	31.3	26.5	15.3
Water	Nitrobenzene	72.8	43.0	0.775	25.2	19.2	23.8
Water	Methylene iodide	72.8	50.8	0.830	48.5	22.6	53.4
Water	Heptylic acid	72.8	28.1	1.0	7.54	10.5	39.8
Water	n-Octanol	72.8	27.5	1.0	8.53	10.9	28.2
Water	sec-Octanol	72.8	26.3	1.0	9.24	11.9	29.3
Water	Caprylic acid	72.8		1.0			

Energy data from references 19 and 22.

Table IV

Test of equation (1). $\epsilon_{ab} = \epsilon_a + \epsilon_b - 2\Phi\sqrt{\epsilon_a \epsilon_b}$

System							
Phase	Phase B	ϵ_a	ϵ_b	Φ	ϵ_{ab} Expt.	ϵ_{ab} Calc.	% Deviation
Water	n-Heptane	119	49.9	0.788	74.3	47.4	36.2
Water	n-Tetradecane	119	52.6	0.682	72.2	86.0	19.1
Water	Benzene	119	69.0	0.875	51.7	30.0	42.0
Water	Ethylene bromide	119	78.2	0.888	68.8	32.0	53.5
Water	Heptylic acid	119	52.6	1.0	19.2	13.4	30.2
Water	n-Octanol	119	50.5	1.0	-3.0	14.5	584
Water	sec-Octanol	119	50.4	1.0	-2.6	14.4	584

Energy data from reference 19

liquid systems is only about 2%, if Φ is taken as unity. As pointed out by Hildebrand and Scott,[20] simplified theoretical models always give better agreement in the free energy than in the total energy. The above results are therefore in accord with expectation. Tables I and II show that $\Phi = 1$ and $\Psi = 1$ are fairly good assumptions for polar-polar systems of about the same molecular size.

Although the theory gives fair results for calculating the ratios Φ and Ψ in terms of molar volumes, provided certain conditions of polarity and geometry are met, it gives poor results when interfacial tension or energy is calculated. As shown by Tables III and IV, equations (54) and (55) are very sensitive to slight errors in Φ and Ψ. Therefore no attempt is made to use (54) and (55) to compute interfacial properties. The main application of the theory is its utilization in obtaining energies of adhesion and estimates of the surface energy of solids.

II. The Contact Angle.

For low energy solid surfaces, equation (70) enables a calculation of the surface free energy from contact angle data.

$$\gamma_s = \frac{\left[\gamma_L(1+\cos\theta)+\pi_e\right]^2}{4\Psi^2\gamma_L} \qquad (70)$$

To test this equation, the free energy of a hydrocarbon surface can be computed from the contact angle of water on a hydrocarbon such as paraffin. Ψ is not accurately given by the molar volume ratio for polar-nonpolar systems, so rather than attempting to calculate it, the experimental value of Ψ for the water-heptane system will be used. From Table II, $\Psi_{H_2O\text{-heptane}} = 0.559$.

Observed values for the contact angle of water on paraffin range from 90° to 110°[23,24]. Zisman et al.[25,26] have reported 88° for water on a stearic acid monolayer and 89° to 102° for an octadecylamine monolayer. In this crude calculation, the contact angle will be taken as 90°, so that $\cos\theta = 0$. γ_L for water is 72.8 ergs/cm.^{2} π_e is generally small for low energy surfaces. For graphite it is about 2 ergs/cm.^{2} (reference 3). Since it would be expected to be even smaller for hydrocarbon surfaces, it will be neglected in this calculation. Using these values, the calculated value for the free energy of a hydrocarbon surface is about 58 ergs/cm.^{2}. The surface tension of liquid hydrocarbons is about 25 ergs/cm.^{2}. Since solids would be expected to have higher surface tensions than liquids, the result of 58 ergs/cm.^{2} is of the right order of magnitude and is consistent with experimental data.

A more reliable check of equation (70) can be obtained by computing values for γ_S from the contact angle of

several liquids on a given solid surface. The contact angles of various liquids on a perfluorolauric acid surface adsorbed on platinum have been measured[27]. For hydrocarbons and halogenated liquids in contact with the adsorbed film, Ψ will be taken equal to unity, and π_e will again be assumed negligible. If the equation in this form is correct, the calculated value of γ_s should be constant for different liquids. Table V shows that equation (70) gives a constant γ_s for twelve different liquids. Furthermore, the surface tensions of liquid perfluorinated hydrocarbons such as C_5F_{12} and C_8F_{18} range from 9 to 14 ergs/cm.^{2} (reference 28). The adsorbed film presents a $-CF_3$ surface to the wetting liquid, and since the surface tension of a $-CF_3$ surface is less than that of a $-CF_2-$ surface[27], the theory gives good results as far as equation (70) is concerned.

III. The Surface Energy of Solids.

The energy of solid surfaces has been estimated by various authors and some of the results will be given here for purposes of comparison.

Using intermolecular potential energy functions, the surface energy has been computed from theory for some solids of simple crystalline form. All such calculations are made by summing the potential energy change per particle pair as the particles approach from infinity to their posi-

Table V

Test of equation (70), $\gamma_s = \frac{[\gamma_L (1+\cos\theta) + \pi_e]^2}{4\Psi^2 \gamma_L}$

for perfluorolauric acid film

Liquid	γ_L	θ	γ_s	% Deviation from Mean
Hexadecane	27.6	78	8.34	4.6
Tetradecane	26.7	76	8.30	5.0
Dodecane	25.4	74	8.10	7.3
Decane	23.9	70	8.03	8.1
Octane	21.8	65	8.00	8.5
$CFCl_2-CF_2-CCl_3$	27.8	66	9.77	11.8
$H(CF_2)_2CH_2OH$	27.6	68	9.49	8.4
p-Difluorobenzene	27.0	66	9.49	8.4
$H(CF_2)_4CH_2OH$	24.5	65	8.73	0.1
$H(CF_2)_6CH_2OH$	23.8	62	8.74	0.0
$CF_2Cl-CCl_2-CF_2Cl$	22.8	49	9.43	7.9
Perfluoroalkane (FCD-330)	20.2	48	8.40	3.9

Mean value for γ_s = 8.74

Average deviation from the mean = 6.2%

tions in the crystal. The results are valid only at 0° K and it is assumed that the solids consist of ideal crystals. As shown by the values in Table VI, the work of different investigators is in serious disagreement and therefore cannot be considered very reliable.

From the nature of the surface energy, it is clear that a finely divided solid will have a greater heat of solution than a large single crystal of the same mass. The excess heat liberated on dissolving the finely divided substance is due to the surface, and this offers another method of obtaining the surface energy. Studies based on this phenomenon have been performed and some of the results are listed in Table VII. Three factors contribute to making these values uncertain. The first is that the difference between the heats of solution of finely divided and bulk material is very small, so that very sensitive calorimetric equipment is required to attain a reasonable degree of accuracy. The second is that most of the work was done before dependable methods were developed for measuring the surface area of solids and the only available method was that of photomicrography. Microscopically measured areas are correct only if the particles are smooth and regular as in the case of spheres or cubes; otherwise the measured area can be considerably in error. Third, finely divided solids may have distorted crystal lattices, and thus not give an energy

representative of the actual crystal planes of the solid. Because of these considerations, much of the earlier work given in Table VII is doubtful. With modern techniques for measuring surface area and using differential microcalorimetry however, the heat of solution method offers an opportunity for direct determination of surface energies.

It is well known that the solubility of a fine powder is greater than the solubility of the corresponding coarse solid. This solubility difference is related to the surface free energy of the solid according to the equation

$$\ln \frac{s}{s_0} = \frac{2\gamma_s}{r\rho} \frac{M}{RT} \qquad (116)$$

s = solubility of a fine powder consisting of spheres of radius r

s_0 = solubility of the coarse solid of negligible area

γ_s = surface free energy of the solid

ρ = density of the solid

M = molecular weight of the solid

R = the gas constant

T = the absolute temperature

Equation (116) can be used to determine the surface free energy of solids. From the variation of γ_s with temperature, the surface total energy can be calculated by the use of the Gibbs-Helmholtz equation.

$$\epsilon_s = \gamma_s + T\frac{\partial \gamma_s}{\partial T} \qquad (117)$$

Such a calculation, however, requires accurately known values of γ_s, and to attain sufficient accuracy, the solid particles must be perfect spheres of accurately known area. Since this condition is never fulfilled for any real solid, equation (116) can give only approximate values of the surface free energy and is worthless for determining the total surface energy. Dundon[29] has carried out such measurements for several salts, and his data is given in Table VIII. His work was performed before dependable methods of measuring surface area were known and so these values must be considered only as rough approximations of the surface free energy.

The bulk of the surface energy values given in the literature therefore are of doubtful value and there really is no way of telling just how accurate they are. However, they can serve as a basis of comparison with the values calculated from heats of wetting, and at least a rough estimate of the consistency of the results can be obtained.

A method of computing surface energy values from heats of wetting is given by equation (62). If the theory is correct, this equation should give a value of ϵ_s for a given solid that is independent of the wetting liquid. For reasons

stated above, this test of the theory has been carried out for systems in which the wetting liquid is of relatively similar polarity to the solid, and assuming that $\Phi = 1$. For purposes of comparison, some surface energy values computed from heats of wetting of liquids dissimilar to the solid have been included. The results of these calculations for high energy surfaces are shown in Table IX. The mean values of the calculated surface energies, using data for different polar liquids, are given in Table X, along with the average deviation from the mean. In Table IX, heats of wetting of polar liquids on polar surfaces are seen to give surface energy values that are in fair internal agreement, except for the case of ethyl alcohol. The reason for this is obscure. All the ethyl alcohol data are from the same literature source and the difficulty might be experimental rather than theoretical. Ethyl alcohol data have not been included in computing the values of Table X. The average deviation from the mean for different liquids on the same solid ranges from 2.5 to 11%. Considering that the heat of wetting and the surface energy of the liquid enter as square terms in equation (62), this can be taken as evidence that the calculated ϵ_s is constant for different liquids on the same solid.

The data of Bartell and Suggitt[30] were used to compute the surface energy of graphite as shown in Table XI. The different calculated surface energies are again in good agreement for systems of non-polar liquids on graphite.

IV. The Interfacial Entropy.

The interfacial entropy of the mercury-benzene system has been reported to be + 0.004 ergs/cm.^{2}/degree. If equation (56) is used to calculate the entropy of the benzene-mercury interface, a value of -0.0075 ergs/cm.^{2}/degree is obtained. In this calculation, Φ and Ψ were computed from the molar volumes as given by equations (57) and (58). Since mercury and benzene have widely different types of potential functions, the ratio $A_{ab}/(A_{aa}A_{bb})^{1/2}$ is probably considerably less than one. This is a possible explanation for the discrepancy between the calculated and observed values. Assuming $A_{ab}/(A_{aa}A_{bb})^{1/2} \simeq 0.8$ gives a calculated interfacial entropy of +0.0065, which is closer to the experimental value. Until more interfacial entropy data becomes available, no decision can be made on the range of validity of equation (56).

Table VI

Theoretical Values for the Surface Energies of Solids in ergs/cm.^{2}

Solid	Surface Energy	Reference
NaF	304	31
NaF	265	32
NaF	176	33
NaF	202	34
NaCl	150	35
NaCl	96	31
NaCl	77	32
NaCl	87	33
NaCl	114	34
NaBr	119	35
NaBr	106	34
NaBr	76	32
NaBr	69	33
NaI	79	32
NaI	88	34
NaI	51	33
KF	180	31
KF	149	32
KF	135	33
KCl	108	35
KCl	77	31
KCl	56	32
KCl	91	33
KBr	92	35
KBr	54	32
KBr	77	33
KI	75	35
KI	58	32
KI	59	33
MgO 100 plane	1360	31
MgO 011 plane	3940	31

Table VI (Continued)

Theoretical Values for the Surface Energies of Solids in ergs/cm.^{2}

Solid		Surface Energy	Reference
MgS	100 plane	357	31
MgS	011 plane	1730	31
CaO	100 plane	1030	31
CaO	011 plane	2850	31
CaS	100 plane	356	31
CaS	011 plane	1440	31

Table VII

Surface Energy Values from Heats of Solution in ergs/cm.^{2}

Solid	Surface Energy	Reference
NaCl	386	36
CdO	500	37
α-Al_2O_3	560	37
CuO	760	37
α-Fe_2O_3	350	37
MgO	1400	38
$Mg(OH)_2$	330	37
Sb_2O_3	140	39
Au	670	40

Table VIII

Surface Free Energy Values from Solubility Measurements in ergs/cm.^{2} - Reference 29

Solid	Surface Free Energy
PbI_2	130
$CaSO_4(H_2O)_2$	370
$AgCrO_4$	575
PbF_2	900
$SrSO_4$	1400
$BaSO_4$	1250
CaF_2	2500

Table IX

Surface Energy Values from Heat of Wetting Data in ergs/cm.^{2} - Calculated from Equation (62)

All values at 25° C. unless otherwise indicated.

Solid	Wetting Liquid	$\epsilon_L - \Delta H_w$	ϵ_s	Reference
$BaSO_4$	H_2O	610	790	41
	H_2O	520 (0°)	575	42
	H_2O	575 (20°)	700	43
	CH_3OH	400 (20°)	800	43
	C_2H_5OH	390 (20°)	760	43
	$n\text{-}C_3H_7OH$	390 (20°)	760	43
	$n\text{-}C_4H_9OH$	385 (20°)	720	43
	$n\text{-}C_4H_9OH$	410	845	43
	$n\text{-}C_6H_{13}OH$	385 (20°)	720	43
	$n\text{-}C_8H_{17}OH$	385 (20°)	720	43
TiO_2 anatase	H_2O	640	860	42
	C_2H_5OH	550	1510	42
	$n\text{-}C_4H_9OH$	400	800	42
	$n\text{-}C_3H_7CO_2H$	455	1050	42
	$C_2H_5OOCCH_3$	420	735	42
	$C_6H_5NO_2$	360	405	42
	CCl_4	300	420	42
	C_6H_6	220	210	42
	$iso\text{-}C_8H_{18}$	155	120	42
TiO_2 rutile	H_2O	900 (0°)	1690	44
	H_2O	670	960	45
SiO_2	H_2O	720	1090	41
	H_2O	1000	2080	46
	H_2O	680	985	45
	C_2H_5OH	570	1620	41

Table IX (Continued)

Surface Energy Values from Heat of Wetting Data in ergs/cm.^{2} - Calculated from Equation (62)

All values at 25° C. unless otherwise indicated

Solid	Wetting Liquid	$\epsilon_l - \Delta H_w$	ϵ_s	Reference
SiO_2	$n\text{-}C_4H_9OH$	470	1110	41
	$CH_3COOC_2H_5$	520	1150	41
	CCl_4	180	150	41
	C_6H_6	220	216	46
	$n\text{-}C_7H_{16}$	230	265	41
ZrO_2	H_2O	720	1100	41
	CCl_4	340	535	41
	C_6H_6	260	290	41
	$iso\text{-}C_8H_{18}$	190	130	41
	$C_6H_5NO_2$	390	485	41
CuO	H_2O	700 (0°)	1000	44
SnO_2	H_2O	800	1330	41
	$n\text{-}C_4H_9OH$	550	1510	41
	$CH_3COOC_2H_5$	590	1450	41
	CCl_4	380	600	41
	C_6H_6	290	300	41
	$iso\text{-}C_8H_{18}$	170	145	41
$ZrSiO_4$	H_2O	970	1980	41
	CCl_4	470	920	41
	C_6H_6	330	400	41
	$iso\text{-}C_8H_{18}$	240	290	41
	$C_6H_5NO_2$	510	810	41

Table IX (Continued)

Surface Energy Values from Heat of Wetting Data in ergs/cm.^{2} - Calculated from Equation (62)

All values at 25° C. unless otherwise indicated

Solid	Wetting Liquid	$\epsilon_L - \Delta H_w$	ϵ_s	Reference
Graphite	H_2O	385	310	41
	C_2H_5OH	300	450	41
	CCl_4	255	300	41
	C_6H_6	285	350	41
Graphon	H_2O	170	62	45
CaF_2	H_2O	1170	2900	46
	CCl_4	160	110	46
	$n\text{-}C_7H_{16}$	225	250	46
ZnS	H_2O	2170	10,000	46
	CCl_4	1360	7,700	46
	$n\text{-}C_7H_{16}$	390	760	46
PbS	H_2O	2750	16,200	46
	CCl_4	185	140	46
	$n\text{-}C_7H_{16}$	635	2,000	46
KCl	CCl_4	185	760	46
	$n\text{-}C_7H_{16}$	390	760	46
$SrSO_4$	H_2O	435 (20°)	400	47
	CH_3OH	250 (20°)	315	47
	$n\text{-}C_8H_{17}OH$	265 (20°)	350	47
$PbSO_4$	H_2O	510 (20°)	545	47
	CH_3OH	370 (20°)	680	47
	$n\text{-}C_8H_{17}OH$	360 (20°)	650	47
$PbCrO_4$	H_2O	440 (0°)	413	48

Table X

Surface Energy Values of Solids - High Energy Surfaces

Temperature	Solid	Surface Energy ergs/cm.^{2}	Number of Liquids used	Average Deviation from the Mean
0°	$BaSO_4$	575	1	---
20°	$BaSO_4$	740	7	3.9%
25°	$BaSO_4$	818	2	3.4%
25°	TiO_2 (anatase)	903	3	10.8%
0°	TiO_2 (rutile)	1690	1	---
25°	TiO_2 (rutile)	960	1	---
25°	SiO_2	1117	3	2.5%
25°	ZrO_2	1100	1	---
0°	CuO	1000	1	---
25°	SnO_2	1420	2	6.3%
25°	$ZrSiO_4$	1980	1	---
25°	CaF_2	2900	1	---
25°	ZnS	10,000	1	---
25°	PbS	16,200	1	---
20°	$SrSO_4$	382	3	10.2%
20°	$PbSO_4$	625	3	8.5%
0°	$PbCrO_4$	413	1	---

Table XI

Surface Energy of Graphite - Using Data of Reference 30

Wetting Liquid	$-\Delta H_w$ ergs/cm.^{2}	ϵ_L ergs/cm.^{2}	ϵ_s ergs/cm.^{2}
C_6H_6	114	69	121
Cyclohexane	101	66.3	105
p-Xylene	124	58.9	142
Hexane	118	49.2	142
n-Octane	120	50.2	139
CCl_4	115	62.9	126
n-BuOH	106	48.5	124
CH_3OH	119	48.8	144
H_2O	47.5	118	56.7

Mean of eight values = 130 ergs/cm.^{2}

Average deviation from the mean = 11.4%

Mean of seven values (not using cyclohexane) = 134 ergs/cm.^{2}

Average deviation from the mean = 8.9%

EXPERIMENTAL

I. Materials

The powders used in this study were: Mallinckrodt's analytical reagent grade copper oxide (CuO) and lead chromate, a laboratory stockroom sample of silica gel, Baker's C. P. aluminum oxide and barium sulfate, Harshaw's bone charcoal, and graphon (L-2808) from Godfrey L. Cabot Inc. Stearic acid was obtained in 99% purity from Emery Industries through the courtesy of J. D. Fitzpatrick. Perfluorodecanoic acid was obtained from the Minnesota Mining and Manufacturing Co.

All water used in the adsorption and wetting experiments was first deionized and then distilled. It had a conductivity less than 5×10^{-6} ohms^{-1}.

Most of the powders were not of sufficient purity, but contained traces of soluble impurities which raised the conductivity of pure water on wetting. These powders were extracted with water to constant conductivity of the wash water, generally in the range of 5×10^{-6} ohms^{-1}. This procedure minimized as far as possible errors in the heats of wetting due to heats of solution.

The above powders were chosen to fulfill the following conditions:

1. The powder must be insoluble in water so that its heat of wetting, rather than a heat of solution is measured.

2. The powder must be available in a finely divided form of high specific surface area so as to give reasonable accuracy in the adsorption and wetting experiments.

3. The powders used should cover a range of surface energies so that a comparison of high energy and low energy surfaces can be made.

4. The powders used should have varying types of particle geometry, so that the effect of porosity and surface heterogeneity on the results could be determined. Thus graphon is spherical, silica and bone charcoal are porous, and the remaining powders are non-spherical and non-porous.

II. The Surface Area of the Powders.

The surface areas of the powders were determined by the nitrogen adsorption methods of Brunauer, Emmett, and Teller[49] and Harkins and Jura[50], and by the gas flow method of Kraus, Ross, and Girifalco[51]. A comparison and detailed discussion of the methods used has been given elsewhere[51,52].

The surface area of the graphon was supplied by Godfrey L. Cabot Inc., along with the sample. The surface area of the aluminum oxide was determined by J. W. Ross at the Applied Science Research Laboratory using the gas flow method. All other areas were determined by the author. The surface area values obtained are given in Table XII.

III. The Adsorption Measurements.

A schematic drawing of the adsorption apparatus, designed both for nitrogen and water vapor adsorption, is shown in Figure IV. The method essentially consists of

Table XII

The Surface Area of Powders

Powder	Surface Area m^2/gm	Method	Surface Area m^2/gm Mean Value
Silica gel	701	BET	701
$PbCrO_4$	3.75	BET	3.83
	4.01	HJ	
	3.73	gas flow	
$BaSO_4$	4.68	BET	4.70
	4.97	HJ	
	4.46	gas flow	
Al_2O_3	7.69	gas flow	7.69
Graphon	95	BET	95
Bone charcoal	245	BET	243
	241	HJ	

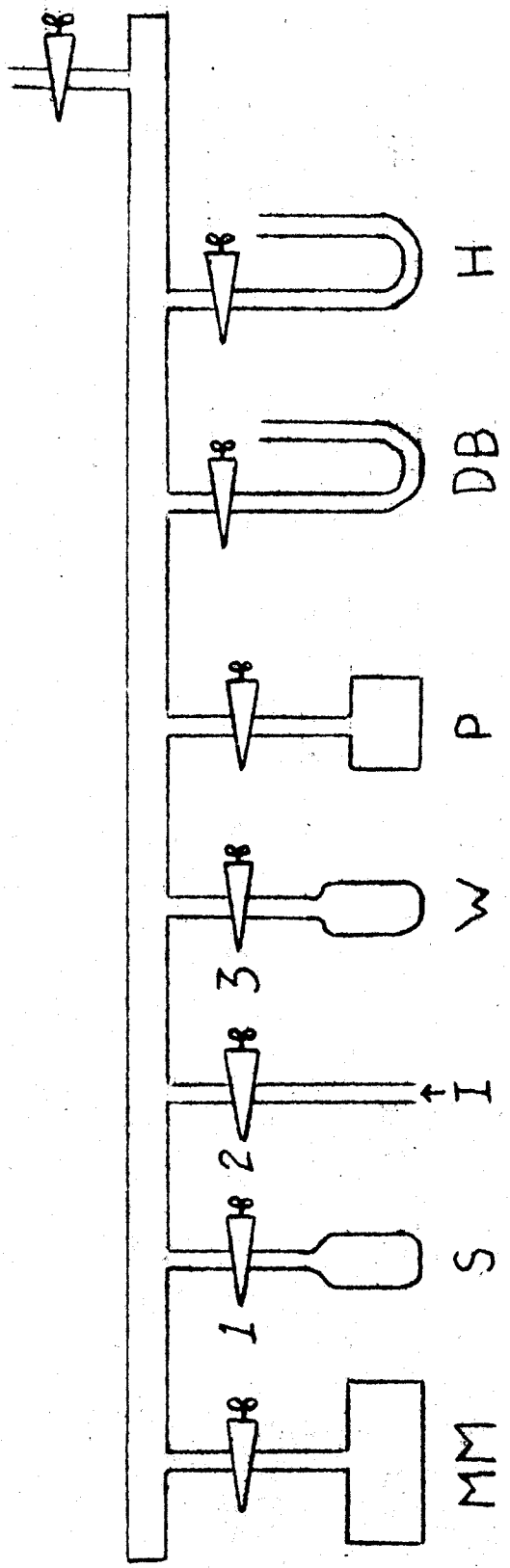

ADSORPTION APPARATUS

FIGURE IV

measuring the pressure in the known volume M both before and after adsorption, and thus computing the amount adsorbed as a function of pressure.

The apparatus is equipped with four pressure gauges: A Pirani gauge P to measure outgassing pressure; a Young and Taylor[53] differential micromanometer MM with a magnification factor of 144; a dibutyl phthalate manometer DB; and a mercury manometer H. In this way, pressures from 0.01 mm. to atmospheric pressure could be measured.

An adsorption isotherm is determined as follows: the powder sample is placed in the bulb S and outgassed at 250° for six hours at less than five microns pressure, with all stopcocks open except 2 and 3. After outgassing, all stopcocks are closed and a constant temperature bath is placed around the sample bulb S. For nitrogen adsorption isotherms, the bath consists of liquid nitrogen. For water vapor adsorption, the bath consists of freezing water glycol mixtures. If nitrogen adsorption is being measured, the desired quantity of nitrogen is admitted from I through stopcock 2. The pressure in the system is then measured with one of the manometers. Stopcock 1 is then opened, thereby allowing the gas to come in contact with the powder in S, and the pressure is again measured. From the two pressures and the dimensions of the apparatus, the amount adsorbed may be calculated. If water vapor adsorption is

being measured, the procedure is the same except that instead of admitting nitrogen from I, water vapor is admitted from the water reservoir W.

IV. Preparation of Powders Containing Preadsorbed Material.

Figure V shows the apparatus used in preparing powder containing a given amount of preadsorbed material.

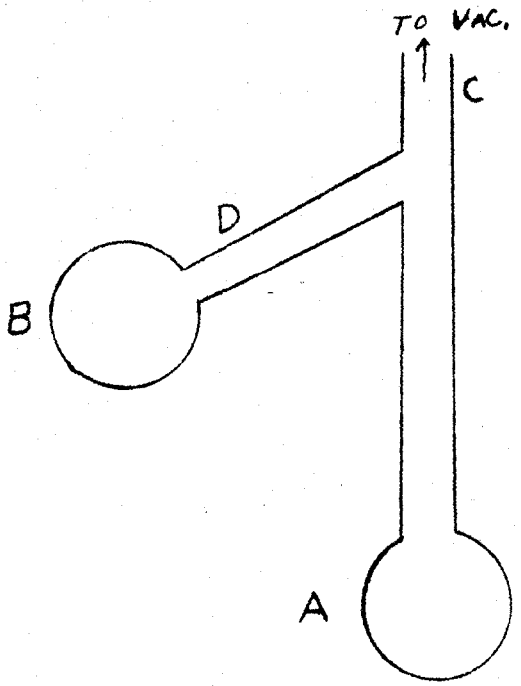

Figure V

The powdered solid is contained in bulb A, and the material to be adsorbed (stearic or perfluorodecanoic acid) in bulb B. A dry ice bath is placed around B and a furnace around A. The system is then pumped down to five microns pressure or less, and the bulb A brought to 250° C. After outgassing for six hours, the glass tube is sealed off with

a torch at C. The powder in A is then transferred to B by tipping, and the bulb B is then sealed off at D. The bulb B, now containing both solid powder and material to be preadsorbed, is placed in an oven a few degrees above the melting point of the preadsorbate for five days. This allows the stearic or perfluorodecanoic acid to distribute itself over the surface of the powder.

The fraction of the surface covered with organic acid can be calculated in two ways. From the specific area of the powder and the weight of organic acid, the fractional coverage can be computed if it is assumed that each acid molecule is standing upright with its carboxyl group at the surface. Then each acid molecule occupies an area equal to the area it would occupy in a close-packed film on a liquid surface. This assumption is probably good for all but the lowest coverages when long-chain acids are used. The cross sectional areas of the acids have been determined experimentally[9].

The second method of computing fractional coverage is to determine the entire heat of wetting versus coverage curve, with the coverage plotted in mgms. per gm. powder. At the completion of a monolayer, there will be no further decrease in the heat of wetting as the coverage increases. Then, assuming that equal weights of acid give equal coverage, the fractional coverage for any given weight of acid

may be calculated from the weight required to complete a monolayer.

In the case of stearic acid, data are available for the molecular cross-sectional area[9], so the two methods can be checked against each other. The results are found to be in fair agreement using a cross-sectional area of 20

V. Calorimetric Measurements.

The magnitude of the heat of wetting is generally of the order of a few calories. In order to attain a reasonable accuracy therefore, an extremely sensitive calorimeter is required. A twin differential microcalorimeter which was built by Berghausen, Fauser, and Buelteman[54,55,56], and modified by Paynter[57], was used in this investigation. The details of the instrument are given in references 54 through 57 and only a brief description will be given here.

In this type of calorimeter, two similar units are used; one for the unknown heat change and the other for the introduction of known heats. Initially, the temperature difference between the two units is set to zero. After the unknown heat is liberated in one of the units, a temperature difference is noted. Known amounts of heat are then added to the other unit until the temperature difference is again zero. If both units are identical, the amount of heat added to the second calorimeter unit is equal to the amount liberated in the first unit. If the two units are not identical addition-

al heating operations can be performed to determine the necessary corrections.

It is not necessary to measure the absolute temperatures or the heat capacities of the calorimeter units. To detect temperature differences, a thermel was used consisting of 125 series connected copper-constantan thermocouples. With the use of auxiliary electronic apparatus, temperature differences as small as a millionth of a degree could be detected.

The powder whose heat of wetting is to be measured is placed in a glass bulb and outgassed at 250° C. for six hours under a pressure of five microns or less. The glass bulb is then placed in one of the twin calorimeter units, both of which contain pure water. A weight is then allowed to fall on the bulb thereby shattering it. The heat of wetting is evolved as the water comes in contact with the powder, and is measured as described above. A certain amount of heat is also evolved due to the breaking of the bulb. Paynter[57] has conducted a detailed study of the heat of breaking by using empty bulbs. For the bulbs used in this investigation the heat of breaking was .25 ± .10 joules, and this amount must be subtracted from every measured heat.

RESULTS AND DISCUSSION

I. The Adsorption Measurements

Adsorption isotherms of water vapor on barium sulfate were determined at -19.2° C. and -25.5° C. The results obtained are given numerically in Table XIII and graphically in Graphs I and II. The curves are typical sigmoid type isotherms in which the initial rate of change of adsorption with pressure is large, the rate of change in the central portion of the curve is small, and the amount adsorbed approaches infinity at the vapor pressure of the liquid. The data are seen to give smooth, consistent curves and indicate that the accuracy of the adsorption measurements is satisfactory.

A plot of the differential heat of adsorption as calculated by equation (17) is shown in Graph III. At low coverage, the heat of adsorption is quite high. As the amount adsorbed increases, the differential heat of adsorption drops very rapidly until monolayer coverage is reached, (5.5×10^{-4} moles adsorbed corresponds to monolayer coverage.) after which it rises and levels off at a value of 12.4 kcal/mole. This is just the heat of sublimation of ice at -20° C. and indicates that the adsorbed water a few molecular layers from the surface has the properties of ice.

The high initial heat may be interpreted as being due to high-energy sites on the solid surface. Water mole-

Table XIII

The Adsorption of Water Vapor on Barium Sulfate

Weight sample = 6.873 grams
Specific Surface Area = 4.70 m^2/gram

Temperature = -19.2° C.		Temperature = -25.5° C.	
Pressure mm. Hg	Moles adsorbed x 10^4	Pressure mm. Hg	Moles adsorbed x 10^4
0.009	1.249	0.000	1.344
0.129	2.534	0.003	2.200
0.137	3.480	0.083	3.096
0.330	4.673	0.274	4.390
0.452	5.423	0.375	5.352
0.528	6.021	0.458	6.357
0.615	6.636	0.468	7.582
0.691	7.308	0.462	8.856
0.816	8.215	0.462	10.077
0.833	9.127		
0.836	10.123		
0.837	11.393		
0.835	13.908		

Graph 1

The Adsorption Isotherm of Water on Barium Sulfate at -19.2° C.

Data Taken From Table XIII

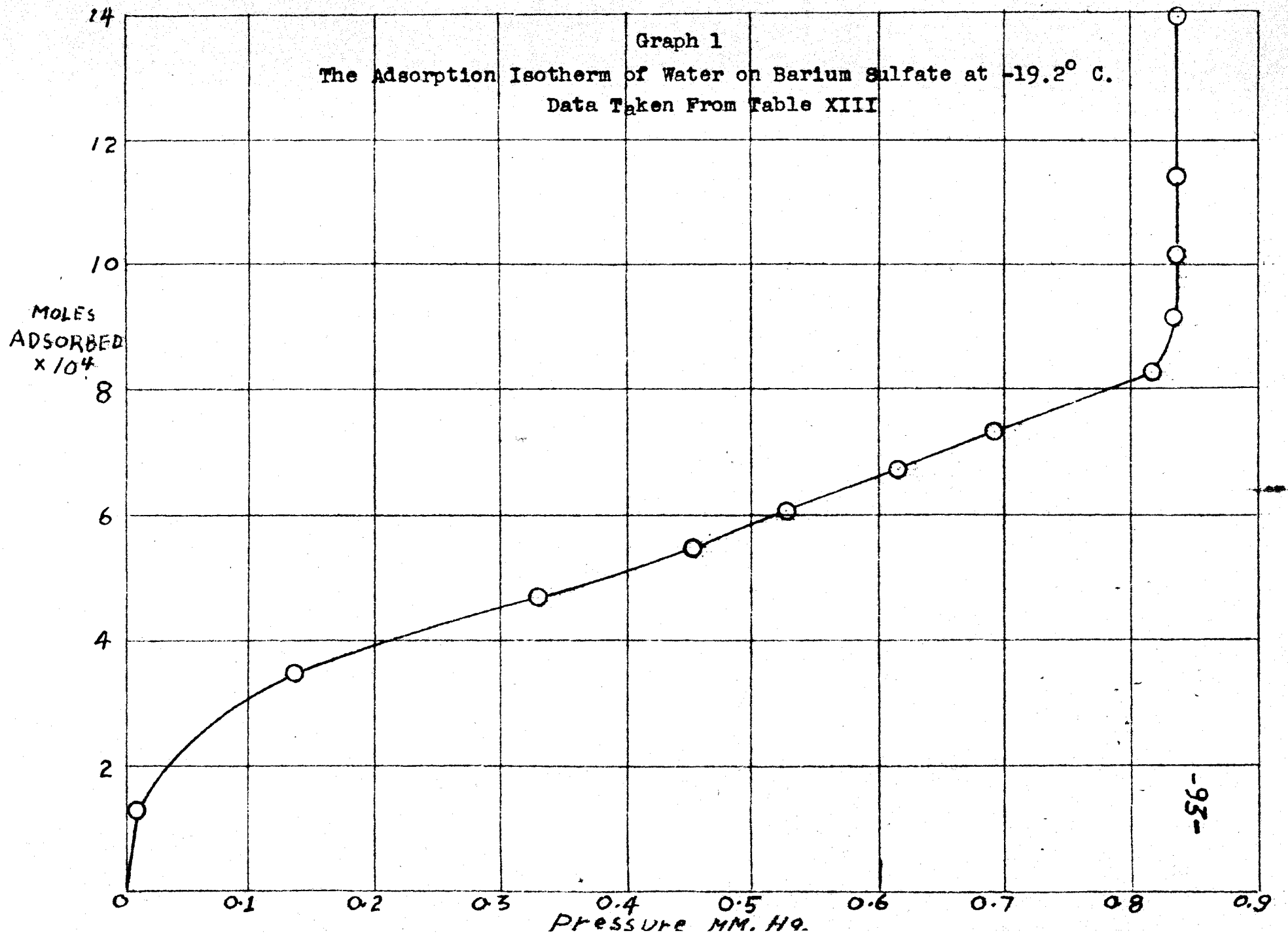

Graph 2

The Adsorption Isotherm of Water on Barium Sulfate at -25.5° C.

Data Taken From Table XIII

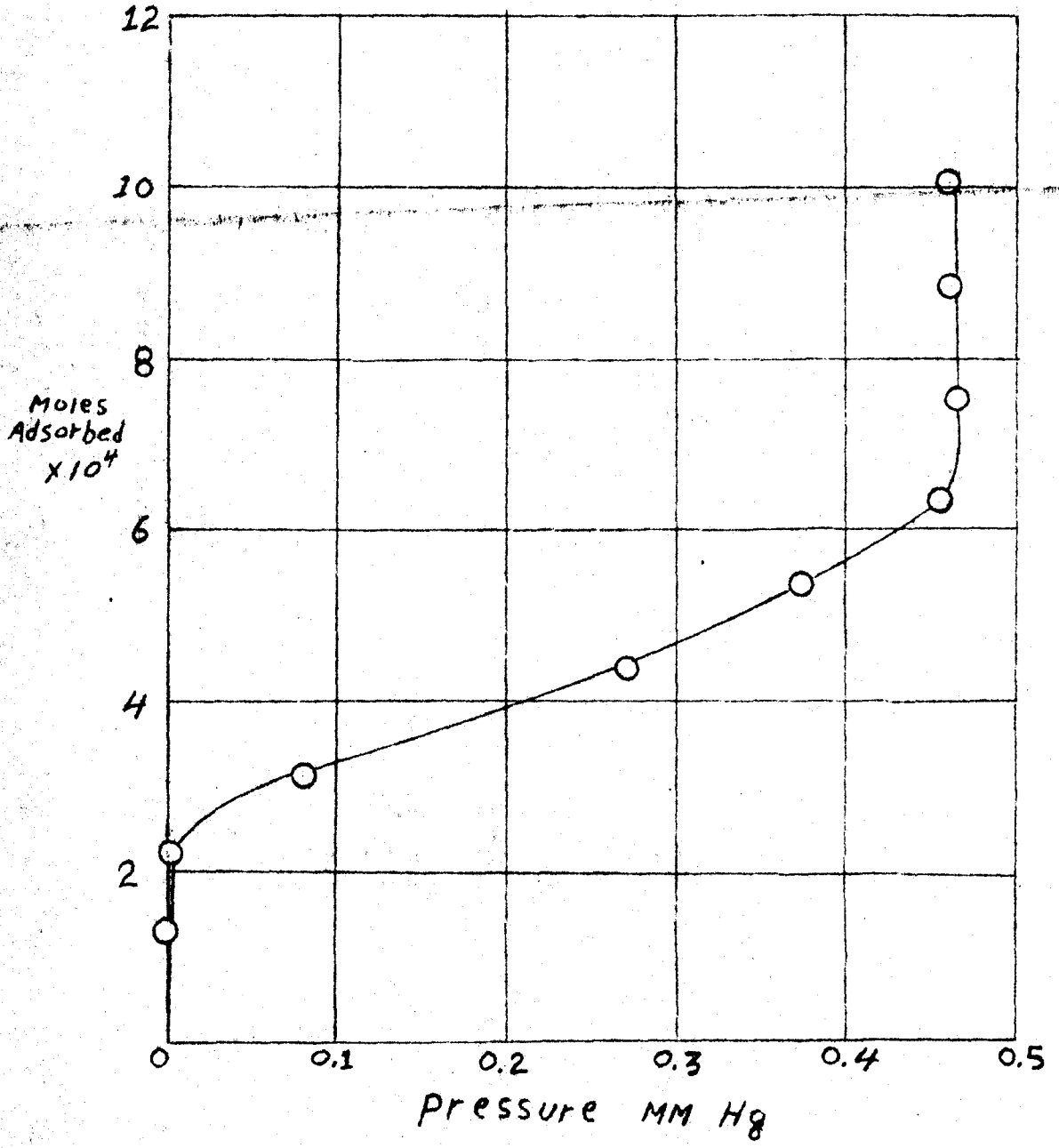

Graph 3

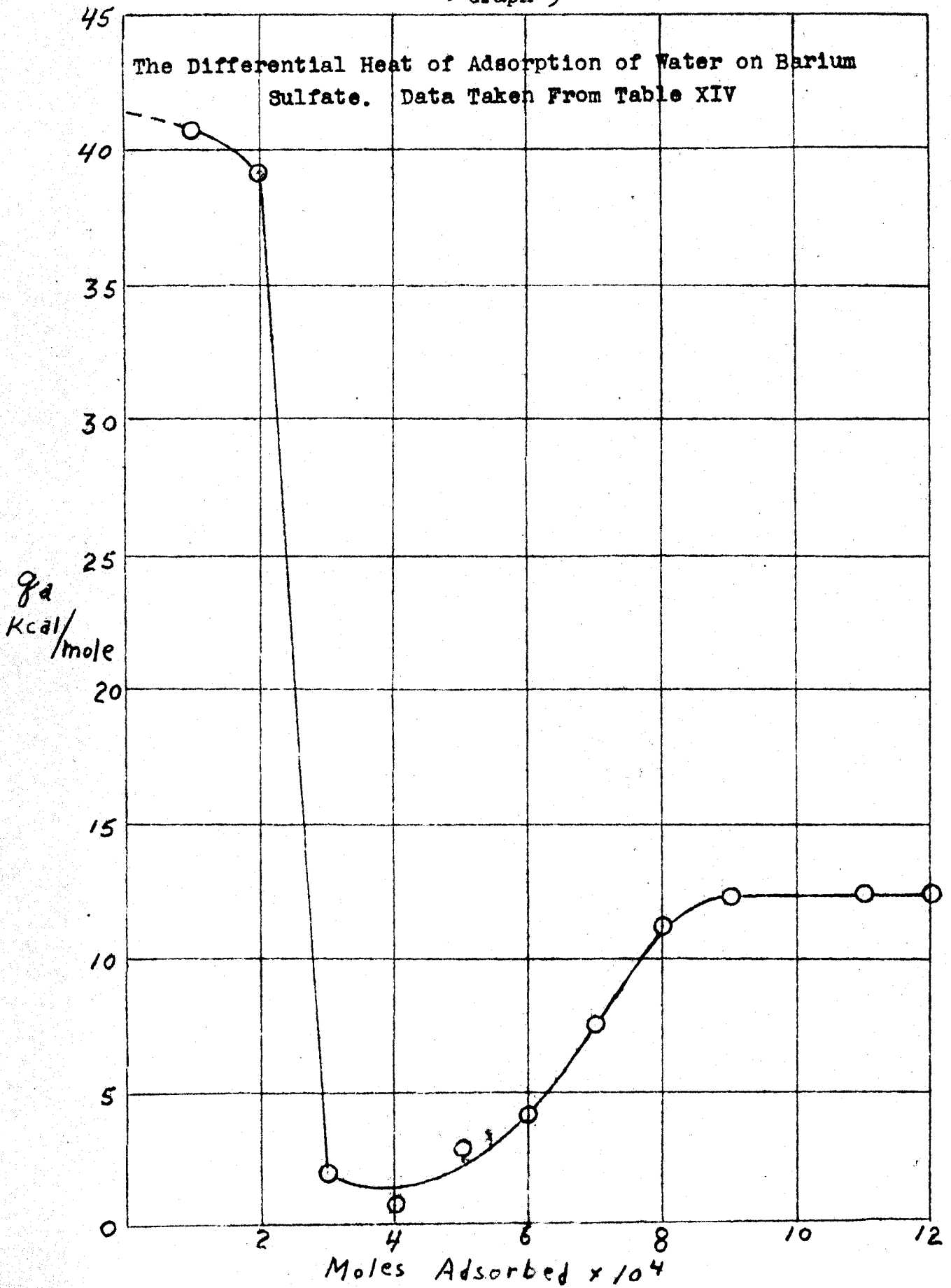

cules are adsorbed on these sites first, thus liberating unusually large amounts of heat in the early stages of adsorption. By the time 40% of the surface is covered, no vacant high-energy sites are left, and adsorption starts taking place at the lower energy sites; thus the heat of adsorption drops rapidly. As the first monolayer nears completion, interactions between adsorbed water molecules become increasingly important. These interactions contribute to the heat of adsorption which therefore rises. As the number of adsorbed layers increases, the adsorption process becomes a condensation process and the heat of adsorption approaches the heat of sublimation. The fact that the curve has a minimum below the heat of sublimation of ice indicates that the first few layers of water molecules do not have the crystalline form of ice, but rather exist in an amorphous liquid-like state. The short-range influence of the surface is therefore very great. However, at a coverage greater than two molecular layers, the surface influence is negligible and the water molecules take on the ice structure.

Graphical integration of the differential heat of adsorption curves gives the integral heat of adsorption as 282 ergs/cm.^{2}

II. The Heat of Wetting and the Energy of Adhesion.

The results of the heat of wetting measurements on clean, dry powders at 0.65° C. are given in Table XIV. Duplicates were run on some of the systems to give an estimate of the accuracy of the method. In general an error of 5-10% can be expected. This error is less in cases where a large amount of heat is evolved and greater where a small amount of heat is evolved. When more than one measurement was performed, mean values were used in subsequent calculations.

The values, -421 ergs/cm.^{2} for the heat of wetting of barium sulfate, 282 ergs/cm.^{2} for the integral heat of adsorption of ice on barium sulfate, and 119 ergs/cm.^{2} for the surface energy of water, were used to compute the surface energy of ice by equation (114). The calculated value of the surface energy of ice is then 172 ergs/cm.^{2}. Using this value for ϵ_I, the adhesion energies of ice to solids were calculated. These results are given in Table XV.

Since these are the first known values for the energy of adhesion of solid-solid systems, no literature data are available which may be used as a basis of comparison with these results. That the results are quite reasonable, however, may be seen from the following considerations. The surface energy of water, 119 ergs/cm.^{2}, is somewhat less than the 172 ergs/cm.^{2} given above for the surface energy of

Table XIV

The Heat of Wetting of Clean Powders at 0.65° C.

Powder	Weight of Sample	Uncorrected Heat	Corrected Heat	Corrected Heat
	gms.	joules	joules/gm.	ergs/cm.^{2}
$BaSO_4$	7.200	-14.50	-1.980	-421
$PbCrO_4$	2.740	-3.86	-1.318	-344
	2.864	-3.60	-1.170	-408
Al_2O_3	4.835	-24.90	-5.15	-670
	4.983	-22.90	-4.54	-591
SiO_2	3.780	-449.5	-118.9	-169
	3.104	-372.9	-120.0	-171
Bone charcoal	3.602	-202.3	-56.2	-231
	3.990	-242.6	-60.9	-250
Graphon	2.391	-6.84	-2.75	-29.0

Table XV

The Adhesion Energy of Ice to Solids

Using = 172 ergs/cm.^{2}; = 119 ergs/cm.^{2}

Solid	ΔE_{rs}^{a} ergs/cm.^{2}
$BaSO_4$	639
$PbCrO_4$	580
Al_2O_3	885
SiO_2	339
Bone charcoal	424
Graphon	174

ice. Since the surface energy of solids can be expected to be above that of liquids, 172 ergs/cm.^{2} is certainly of the correct order of magnitude for the surface energy of ice. Also, the polar hydrophilic solids have a high energy of ice adhesion, while the non-polar hydrophobic graphon surface has a low energy of ice adhesion. This is entirely in line with general expectations.

Beyond the general consistency of these data with known facts, no more specific check on the results can be made because of the lack of literature data on the subject.

III. The Heat of Wetting as a Function of Preadsorbed Material and Surface Heterogeneity.

Measurements of the heat of wetting as a function of the amount of preadsorbed material were carried out on lead chromate and aluminum oxide. On lead chromate, two different preadsorbates were used; perfluorodecanoic acid and stearic acid. On aluminum oxide, stearic acid was used as the preadsorbate. The results of the heat of wetting measurements are given in Tables XVI, XVII, and XVIII and in Graphs 4, 5, and 6. (For convenience, these tables and graphs are collected at the end of this section.)

Using the value 20.5 Å^2 for the cross-sectional area of the stearic acid molecule, monolayer coverage for stearic acid corresponds to 2.31×10^{-4} mg. of stearic acid per $cm.^2$ of surface. This value was used in calculating θ, the fraction of the surface covered.

No cross-sectional area values for perfluorodecanoic acid are available in the literature. At a coverage of 2.0×10^{-4} mg. of perfluorodecanoic acid per $cm.^2$ of surface, the heat of wetting of lead chromate was observed to become zero, as may be seen from Graph 4. Furthermore, increasing the coverage does not change the heat of wetting. This coverage was therefore assumed to correspond to a monolayer; i.e., $\theta = 1$. The cross-sectional area calculated from this value is 42.5 Å^2, which is about twice the cross-sectional area of stearic acid. While the cross-sectional area

of the perfluoro acid would be expected to be considerably larger than that of stearic acid, the value 42.5 $\mathring{A}^2$ is probably too high. The heat of wetting method does not give an unequivocal value for the area per molecule of perfluorodecanoic acid, but the value is well within the right order of magnitude. Examination of Graph 4 shows that if the point at 1.86×10^{-4} mg. per cm.^{2} surface were too low, the curve could be drawn in such a way that zero heat of wetting would not be attained until a coverage of 2.7×10^{-4} mg. per cm.^{2} were reached. This would correspond to a cross-sectional area of 31.5 $\mathring{A}^2$.

At any rate, until independent data on the cross-sectional area of perfluorodecanoic acid becomes available, no course can be empirically justified other than taking monolayer coverage to correspond to 2.0×10^{-4} mg. per cm.^{2} surface. As long as the same curve is used in computing both monolayer coverage and the values of $\bar{h}$, the errors in the final curve of ϵ_s vs. θ are not likely to be great.

With the values of θ calculated on the basis of the above values for monolayer coverage, $\bar{h}$, the heat of wetting due to the bare part of the surface, and ϵ_s, the surface energy at θ coverage, were calculated from the smoothed out curves using equations (75) and (80). The derivative $\frac{d\bar{h}}{d\theta}$ was computed graphically from a plot of $\bar{h}$ vs. θ. The results of these calculations are shown in

Tables XIX, XX, and XXI, and in Graphs 7, 8, 9, 10, and 11.

Graphs 4 and 5 show that perfluorodecanoic acid and stearic acid are equally effective in lowering the heat of wetting of lead chromate, up to about 10 mg./cm.^{2} surface coverage. Beyond this coverage, perfluorodecanoic acid is more effective than stearic acid in lowering the heat of wetting. The stearic acid monolayer has a heat of wetting of about 40 ergs/cm.^{2} whereas the perfluorodecanoic acid has a zero heat of wetting. This is in accord with the observation made in a previous section that hydrocarbon surfaces have a considerably higher energy than perfluoro surfaces.

The heat of wetting curve for aluminum oxide, shown in Graph 6, is seen to be of the same general form as the curves for lead chromate. Several discrepancies should be noted, however. A comparison of Graphs 5 and 6 shows that the same amount of stearic acid, at low coverages of acid, produces a considerably greater drop in the heat of wetting of aluminum oxide than in that of lead chromate. This indicates that a smaller percentage of the sites on the alumina surface have very high energy. On the lead chromate surface, the same amount of energy is distributed over a greater number of sites. This conclusion is verified by the surface energy distribution curves of Graphs 10 and 11.

The curve of Graph 6, for stearic acid on alumina, was the only one that showed a slight, but definite, rise

after the completion of a monolayer. This rise could be due to adsorption in the second layer taking place in such a way that carboxyl groups are sticking outward rather than hydrocarbon chains. Why this phenomenon was not observed in the lead chromate systems is not clear. The specific surface area of the lead chromate was about half that of the aluminum oxide. The same rise in the heat of wetting of the lead chromate samples would be twice as difficult to detect, so it is possible that experimental error masked a slight rise in the heat of wetting.

The heat of wetting of the lead chromate systems levels off at the expected monolayer coverage of acids. In the alumina system, however, the heat of wetting becomes constant at only about 35% of the monolayer coverage. A possible explanation of this is given below.

Graphs 5 and 6 show that the heat of wetting of stearic acid adsorbed on lead chromate is about 40 ergs/cm.^{2}, but the heat of wetting of stearic acid adsorbed on alumina is about 75 ergs/cm.^{2}. The stearic acid molecule is long enough so that the ends of the hydrocarbon chains are far removed from the influence of the surface. A stearic acid film therefore would be expected to give the same heat of wetting regardless of the nature of the underlying substrate. The heats of wetting for powders containing large amounts of stearic acid were quite small, and it is possible that the

experimental error of these low heats is sufficient to account for the discrepancy. The facts that the heats of wetting were fairly constant with coverage in this region, and that the scatter of the points was not sufficiently great to cover a band of 70 ergs/cm.^{2} in width seem to argue against this possibility. An alternative explanation might be that the films formed were not of tight enough packing to prevent some diffusion of water molecules to the surface. Aluminum oxide is much more basic than lead chromate. Thus in approaching the alumina surface a stearic acid molecule could liberate a proton which could migrate into the aluminum oxide. The basic alumina surface could then repel the stearate ion and the film would then be loosely packed. If this repulsion were strong enough, an inversion could occur such that the stearate ion would be adsorbed with its hydrocarbon towards the surface and its carboxylate ion away from it. Both the loosening of the film and the inversion of adsorption orientation would lead to heats of wetting higher than the heat of wetting of a stearic acid monolayer. These effects would not be expected on the relatively nonbasic lead chromate surface, so the results would be as indicated in Graphs 5 and 6.

Graphs 7, 8, and 9 give the distribution functions for the heat of wetting on lead chromate and aluminum oxide. For lead chromate, two curves were computed, one from heat

of wetting data using perfluorodecanoic acid and the other stearic acid as the film forming substance. The method of calculation is such that the results should be independent of the nature of the film and, since the substrate is the same in both cases, Graphs 7 and 8 should be identical. Actually, the two curves differ considerably. Part of this difference is certainly due to the inaccuracies inherent in choosing values for monolayer coverage and in drawing the proper curve to fit the original heat of wetting data. The greatest discrepancy is seen to exist for values of θ below 0.25; i.e., at low coverages of organic acid. In computing θ, it was assumed that each acid molecule stood upright and covered an area on the surface equal to its cross-sectional area. At low coverages this assumption may be inaccurate. It is more probable that the long-chain molecules either lie flat on the surface or are tilted at an appreciable inclination from the normal. In either case, each molecule would cover more area than if it were standing upright. In the flat or tilted configuration, the longer the chain, the greater the area that would be covered. Hence, the longer the chain length of the acid, the greater the reduction in the heat of wetting by a given number of molecules. The curves show that at low coverages stearic acid is more effective than perfluorodecanoic acid in decreasing the heat of wetting as required by this hypothesis.

Graph 9 gives the distribution function for the heat of wetting of aluminum oxide. The heat of wetting is seen to become constant after a value of $\theta = 0.4$ is reached.

Graph 10 gives the surface energy distribution for lead chromate, using two different preadsorbates in the measurements. The two sets of data were computed from Graphs 7 and 8. The agreement between the two sets of data is good, especially considering the experimental difficulties involved and the approximations and errors inherent in the calculations. The difference noted above between the results obtained with perfluorodecanoic acid and stearic acid still exist but to a lesser degree. As shown by the distribution curve, only a small part of the lead chromate surface has a very high energy: only 10% of the surface has energy above 1100 ergs/cm.^{2} and only 20% has energy above 500 ergs/cm.^{2}. About 60% of the surface has energy less than 200 ergs/cm.^{2}. The surface of lead chromate therefore is quite heterogeneous in that sites having energies of greatly differing magnitudes are present.

The distribution of surface energy for aluminum oxide is shown in Graph 11. About 40% of this surface is highly heterogeneous, and sites of greatly varying energies are present. The curve indicates that the remaining 60% of the surface, however, has a constant energy of 77 ergs/cm.^{2}. The alumina surface therefore is more homogeneous in its

homogeneous portion, and more heterogeneous in its heterogeneous portion, than the lead chromate surface.

These data provide an interpretation for the fact that the heat of wetting of the aluminum oxide system levels off at 35% of monolayer coverage. The value of 77 ergs/cm.^{2} is only a little higher than the surface energy of a hydrocarbon surface previously computed from contact angle data. If the preadsorbed film and the bare part of the surface have the same surface energy, the heat of wetting would be constant with coverage.

It would seem surprising, however, that an Al_2O_3 surface should have such a low energy. Alumina is known to have a great affinity for water and it is possible that a hydrate was formed on part of the surface that was not decomposed during the outgassing procedure. The chemisorbed water would be expected to lower the surface energy and smooth out surface heterogeneities. Thus it would be expected that the low value of 77 ergs/cm.^{2} corresponds to a hydrated surface and not to the substance Al_2O_3.

The experimental levelling off of ϵ_s vs. θ for aluminum oxide is believed to be real for the following reasons:

1. The error due to loose packing of the film, or the presence of "inverted" stearate ions is subtracted out by the method of calculation.
2. A large error in the surface area of the alumina is unlikely.

3. Chemisorbed water would tend to lower the surface energy and smooth out heterogeneities.

The presence of chemisorbed water leads one to expect that the homogeneous portion of alumina would be more homogeneous than the homogeneous portion of lead chromate. Alumina is prepared by dehydration of a hydrate, and lead chromate by precipitation from solution. As a result, the lead chromate crystals are more homogeneous and more perfectly formed than those of alumina. Because of this it is to be expected that the heterogeneous portion of the alumina would be more heterogeneous than the heterogeneous portion of lead chromate.

It is evident from these curves that the high energies of ice adhesion for alumina and lead chromate, listed in Table XV, are largely the result of about 30% of the available surface having energy greatly in excess of the average value. Most of the ice is bound to the surface rather loosely, but the presence of some very high energy sites results in a fraction of the surface being attached to the ice by very strong bonds. As noted above, the first few layers of water molecules no doubt exist in an amorphous rather than crystalline condition, so that the contribution of the ice to the adhesion energy may be considered as constant over the surface. Because of this, the distribution function for the energy of ice adhesion would be expected to have the same form as Graphs 10 and 11.

It is fairly certain that the results just given represent correctly the general form of the energy distribution of the lead chromate and aluminum oxide surfaces. Because of the theoretical and experimental limitations inherent in the method, the absolute values of the surface energy distribution are only approximate. The experimental difficulties alone could probably lead to an error as great as 10%. It was assumed in this work that Φ was equal to unity. A 5% error in this assumption gives a 10% error in the surface energy values, since Φ enters as a square term in the equation for the surface energy. On account of this and the other approximations discussed above it is felt that the energy values in curves 10 and 11 should not be taken too literally. Rather, the curves indicate the expected magnitude of surface energy and the general trend of the distribution function.

In spite of their approximate nature, the results are valuable in that they are the first direct measurements of surface heterogeneity. The distribution of surface energy has been investigated previously by means of adsorption experiments[10]. The differential heat of adsorption was plotted against the amount of gas adsorbed and, by assuming that all differences in the differential heats were due to differences in the solid surface, a distribution function was computed. A serious limitation to this procedure is that

adsorbed molecules interact with each other as well as with the surface. Thus at all but the lowest coverages, the heat of adsorption includes not only the energy of interaction with the surface, but also the energy of interaction between adsorbed gas molecules. The heat of wetting method is not subject to this limitation since the heat of wetting is an integral property and interactions between water molecules is only very slightly involved in the wetting process.

Table XVI

The Heat of Wetting as a Function of Preadsorbed Perfluorodecanoic Acid on $PbCrO_4$ at 0.65° C.

Specific Surface Area = 4.82 $m.^2/gm.$

Weight $PbCrO_4$ gm.	PFA mg.	PFA per $cm.^2$ surface x 10^4	Uncorrected Heat joules	Corrected Heat* joules/gm.	Corrected Heat* $ergs/cm.^2$
2.740	0.00	0.00	3.862	1.32	344
2.864	0.00	0.00	3.604	1.17	408
5.014	1.54	0.08	5.409	1.03	268
5.009	8.64	0.450	2.583	0.465	121
4.989	15.05	0.788	1.917	0.335	87
4.966	35.46	1.861	0.178	-0.014	- 4
5.017	53.50	2.79	0.125	-0.024	- 6
5.005	70.67	3.69	0.631	0.076	20
4.977	73.50	3.86	0.121	-0.026	- 7
5.002	102.23	5.35	0.563	0.062	16
4.103	104.59	6.66	0.095	-0.037	- 10

* 0.25 jourles was the heat of breaking, so this value was subtracted from the uncorrected heat, and the result used in computing the corrected heat per gram and per $cm.^2$.

Table XVII

The Heat of Wetting as a Function of Preadsorbed Stearic Acid on $PbCrO_4$ at 0.65° C.

Specific Surface Area = 4.82 $m.^2/gm.$

Weight $PbCrO_4$ gm.	SA mg.	SA per $cm.^2$ surface x 10^4	Uncorrected Heat Joules	Corrected Heat Joules/gm.	Corrected Heat $ergs/cm.^2$
2.740	0.00	0.00	3.862	1.32	344
2.864	0.00	0.00	3.604	1.17	408
4.991	0.64	0.034	3.838	0.720	188
5.004	7.57	0.396	2.861	0.522	136
4.993	14.52	0.760	1.528	0.257	67
5.003	30.62	1.599	1.799	0.310	81
5.007	51.62	2.70	1.131	0.176	46
4.999	71.72	3.75	0.883	0.126	33
5.006	92.96	4.85	-0.008	-0.052	-14
5.048	106.13	5.50	1.192	0.186	49

Table XVIII

The Heat of Wetting as a Function of Preadsorbed Stearic Acid on Al_2O_3 at 0.65° C.

Specific Surface Area = 7.69 $m.^2/gm.$

Weight Al_2O_3 gm.	SA mg.	SA per $cm.^2$ surface $\times 10^4$	Uncorrected Heat joules	Corrected Heat joules/gm.	Corrected Heat $ergs/cm.^2$
4.835	0.00	0.00	24.9	5.15	670
4.983	0.00	0.00	22.9	4.54	591
4.98	3.95	0.103	7.32	1.42	185
4.93	8.51	0.225	7.59	1.49	194
5.03	7.29	0.189	3.74	0.70	91
4.98	14.1	0.368	4.85	0.92	120
5.02	23.2	0.601	3.49	0.65	84
5.02	31.1	0.808	3.10	0.57	74
4.98	35.0	0.915	4.75	0.90	118
5.13	46.1	1.170	3.11	0.55	72
5.10	59.0	1.508	3.15	0.57	74
5.05	64.9	1.670	1.78	0.30	39
5.02	76.9	1.990	3.19	0.59	76
5.00	81.4	2.22	3.42	0.63	82
5.01	98.6	2.57	4.01	0.75	98
4.99	102.4	2.68	3.52	0.66	85
5.04	109.1	2.82	4.80	0.90	118

Table XIX

The Surface Energy Distribution of $PbCrO_4$ Calculated from the Heat of Wetting, as a Function of Preadsorbed Perfluorodecanoic Acid, at 0.65° C.

θ	$-\Delta H_w$ ergs/cm.^{2}	$-\bar{h}$ ergs/cm.^{2}	$\frac{d\bar{h}}{d\theta}$	ϵ_s ergs/cm.^{2}
0.0	380	380	3170	7200
0.05	290	305	1212	2445
0.10	220	245	852	1450
0.20	150	187	448	662
0.30	105	150	350	411
0.40	70	117	288	287
0.60	27	68	213	139
0.80	5	25	162	62
1.00	0	0	110	30

Table XX

The Surface Energy Distribution of $PbCrO_4$ Calculated from the Heat of Wetting, as a Function of Preadsorbed Stearic Acid, at 0.65° C.

θ	$-\Delta H_w$ ergs/cm.^{2}	$-\bar{h}$ ergs/cm.^{2}	$\frac{d\bar{h}}{d\theta}$	ϵ_s ergs/cm.^{2}
0.05	190	198	1435	2030
0.10	154	167	502	755
0.20	109	125	250	329
0.30	89	109	172	223
0.40	73	93	115	155
0.60	56	75	94	110
0.80	48	70	74	86
1.00	43	43	57	55

Table XXI

The Surface Energy Distribution of Al_2O_3 Calculated from the Heat of Wetting, as a Function of Preadsorbed Stearic Acid, at 0.65° C.

θ	$-\Delta H_w$ ergs/cm.^{2}	$-\bar{h}$ ergs/cm.^{2}	$\frac{d\bar{h}}{d\theta}$	ϵ_s ergs/cm.^{2}
0.05	310	322	3335	6275
0.10	170	181	1270	1630
0.20	102	109	372	395
0.30	88	94	168	201
0.40	73	73	68	111
0.60	73	73	0	77
0.80	73	73	0	77
1.00	73	73	0	77

Graph 4

The Heat of Wetting of Lead Chromate as a Function of the Amount of Preadsorbed Perfluorodecanoic Acid

Data Taken From Table XVI

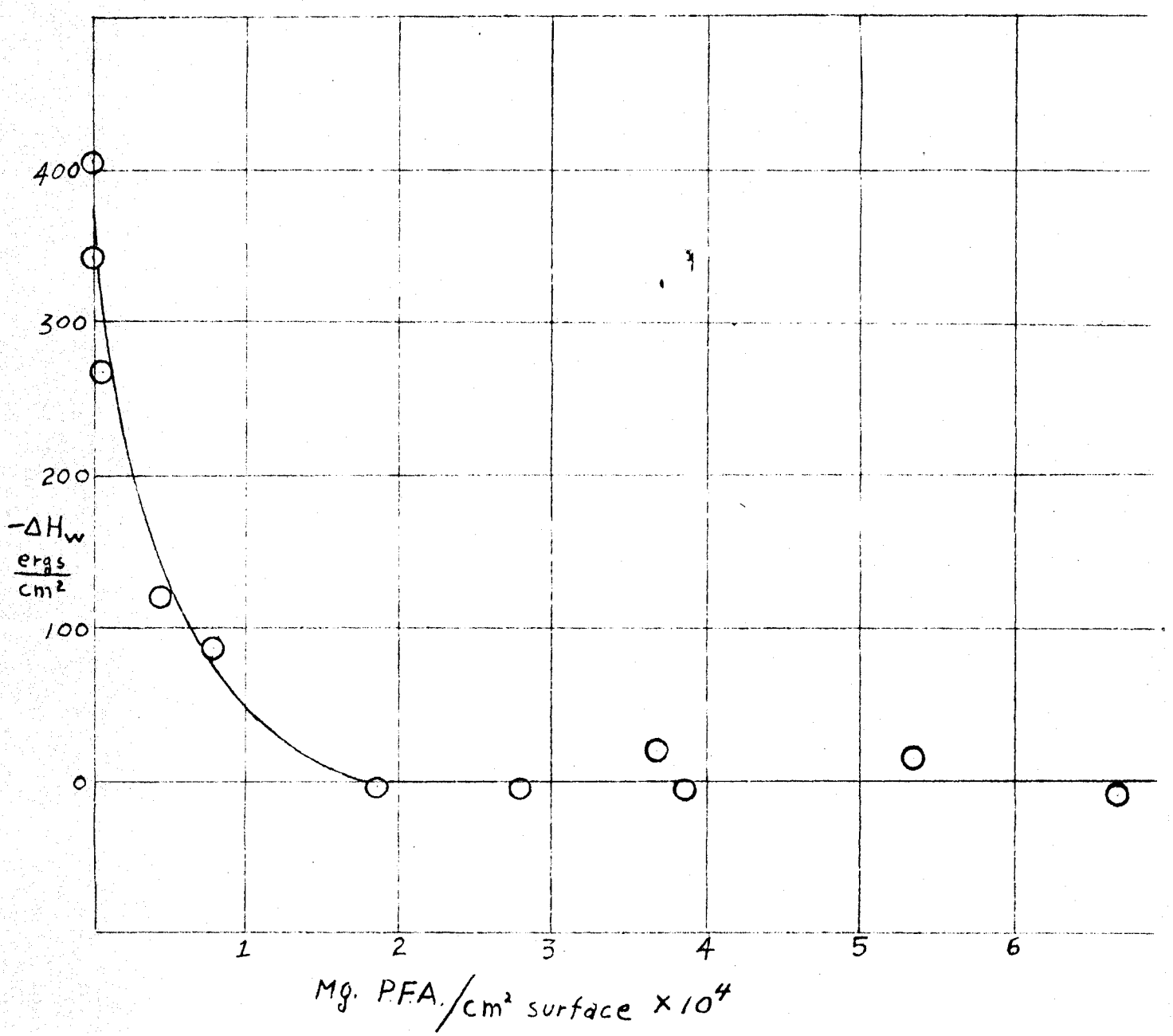

Graph 5

The Heat of Wetting of Lead Chromate as a Function of the Amount of Preadsorbed Stearic Acid

Data Taken From Table XVII

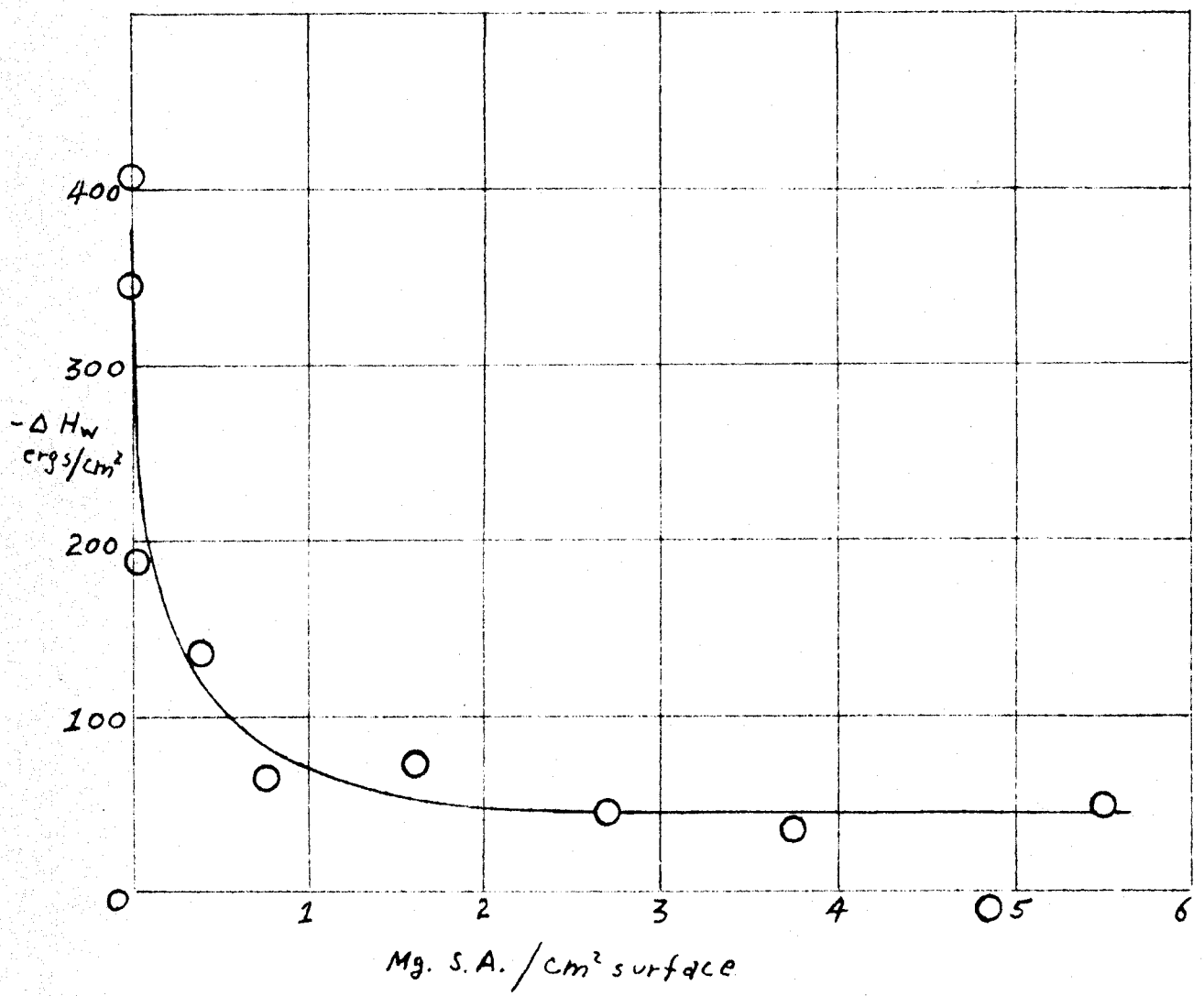

Graph 6

The Heat of Wetting of Aluminum Oxide as a Function of the Amount of Preadsorbed Stearic Acid

Data Taken From Table XVIII

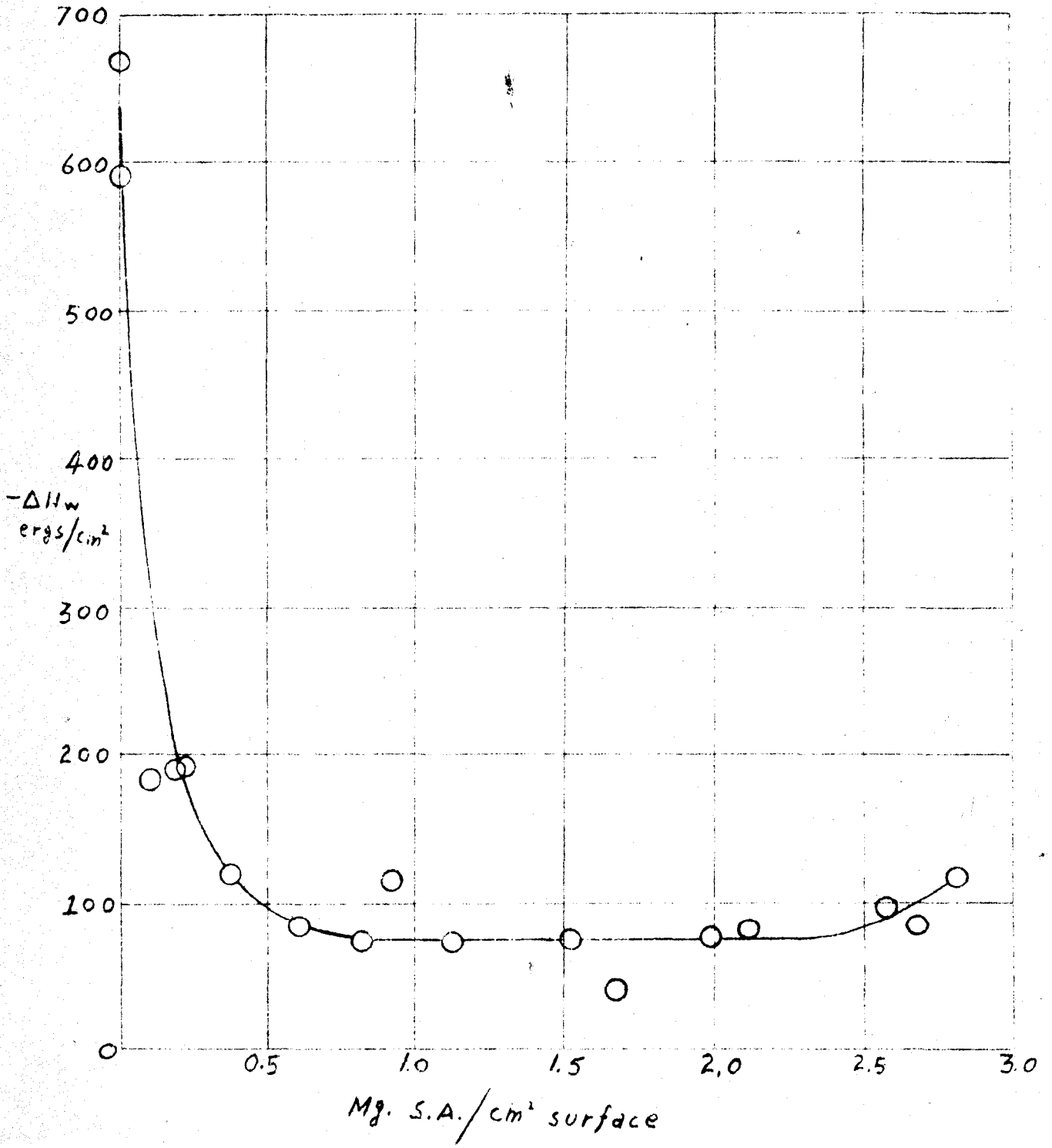

Graph 7

The Contribution of the Bare Part of the Surface to the Heat of Wetting of Lead Chromate Containing Preadsorbed Perfluorodecanoic Acid. Data Taken from Table XIX

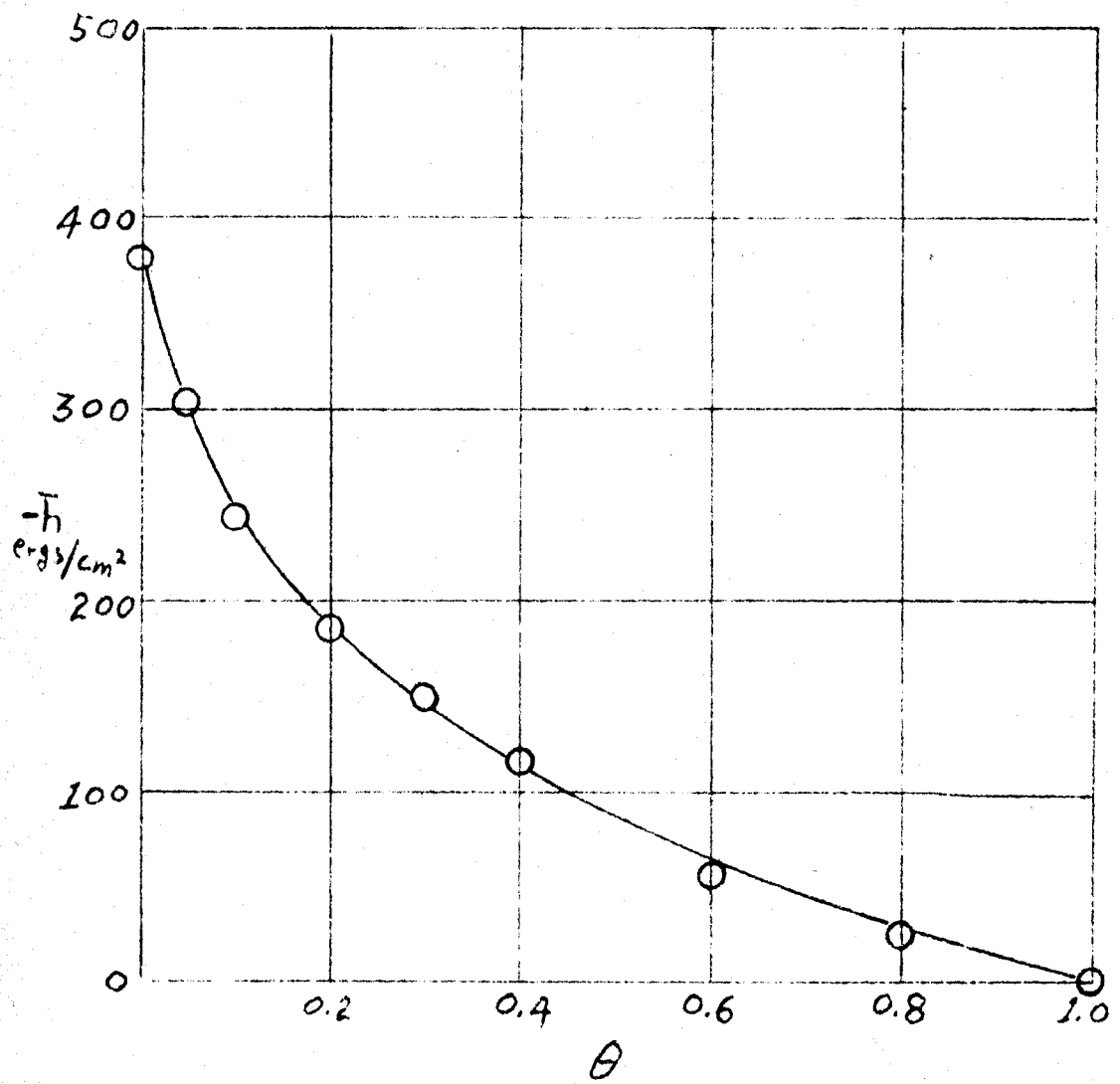

Graph 8

The Contribution of the Bare Part of the Surface to the Heat of Wetting of Lead Chromate Containing Preadsorbed Stearic Acid. Data Taken From Table XX.

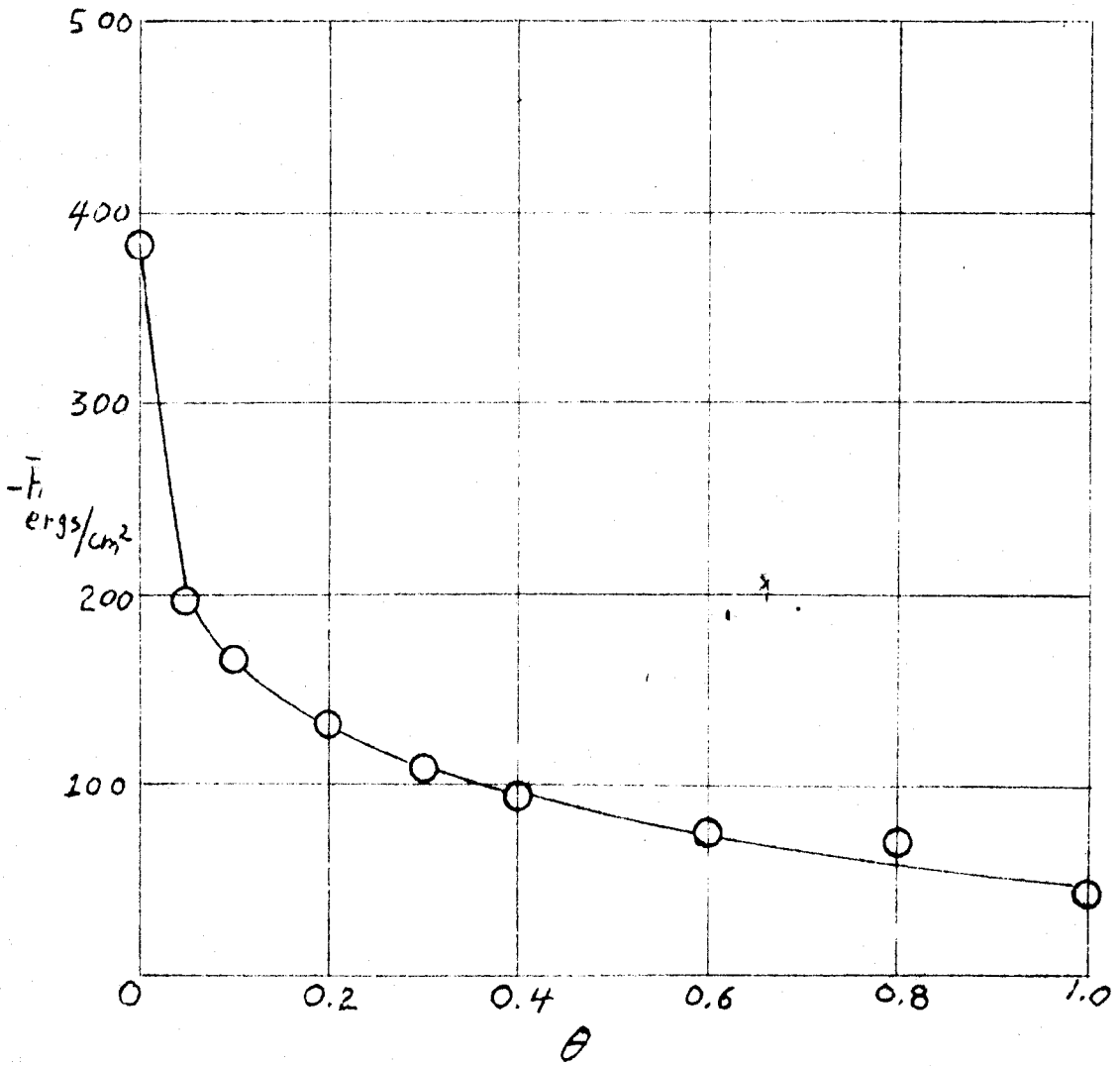

Graph 9

The Contribution of the Bare Part of the Surface to the Heat of Wetting of Aluminum Oxide Containing Preadsorbed Stearic Acid. Data Taken From Table XXI

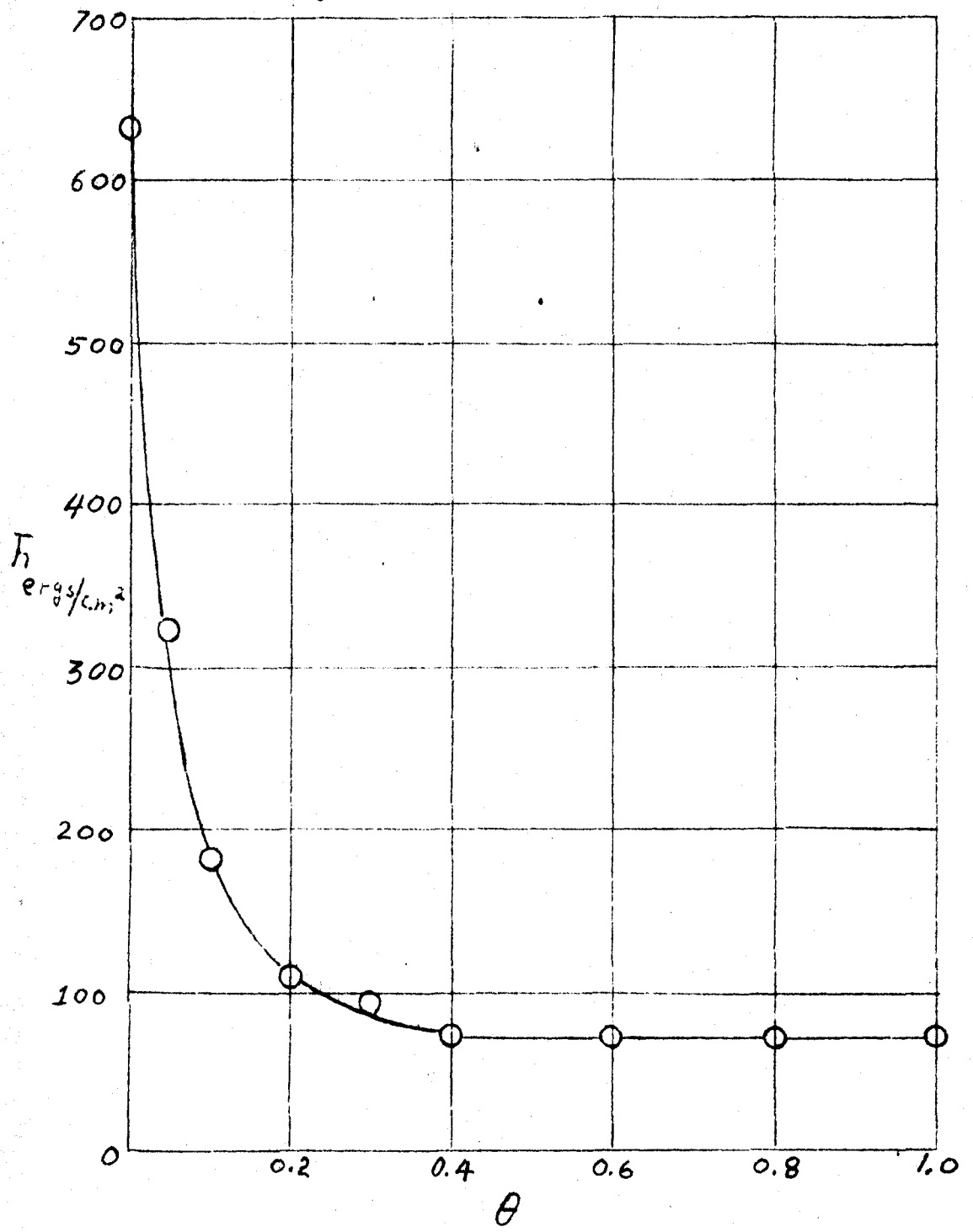

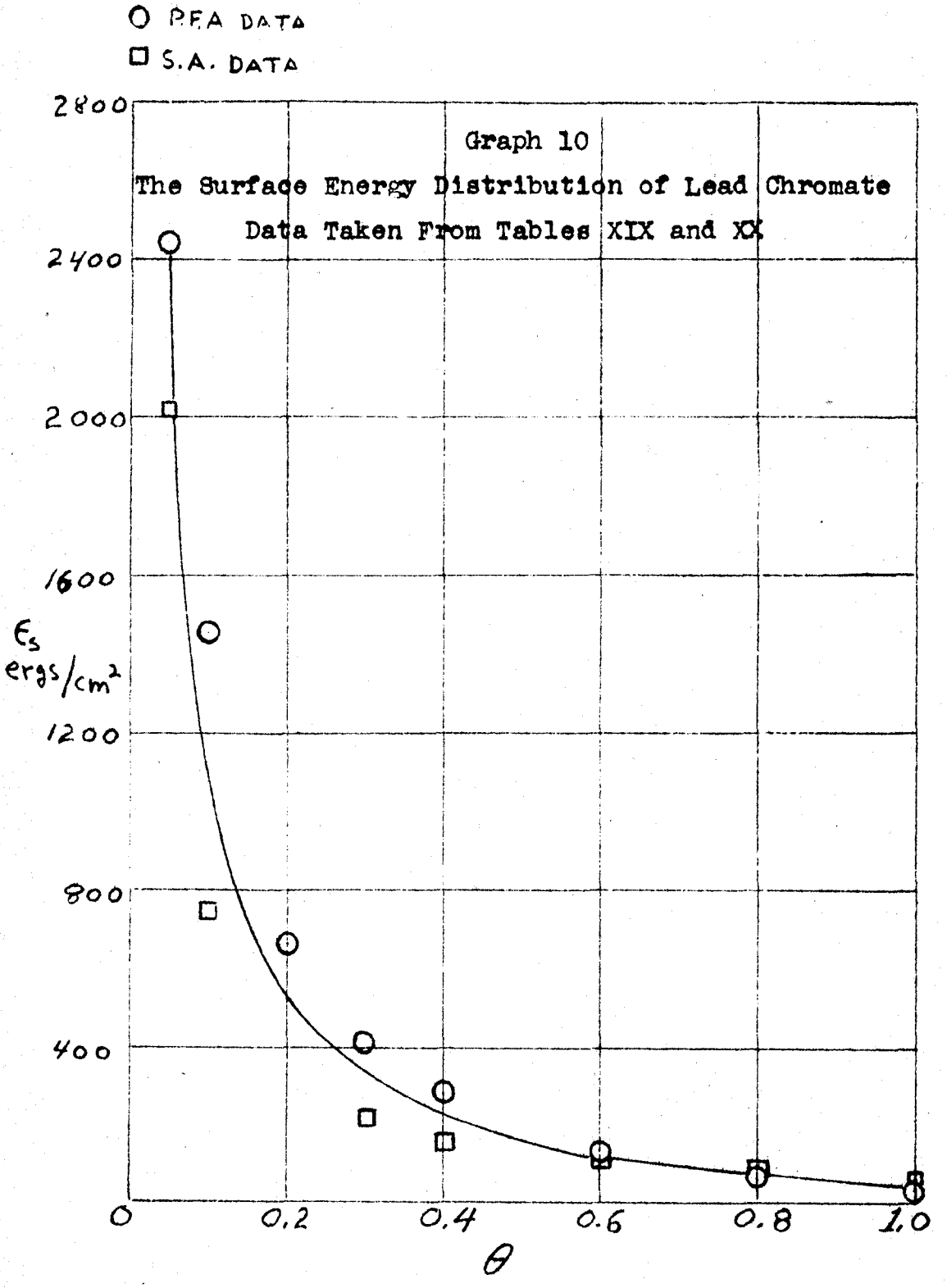

Graph 11

The Surface Energy Distribution of Aluminum Oxide

Data Taken From Table XXI

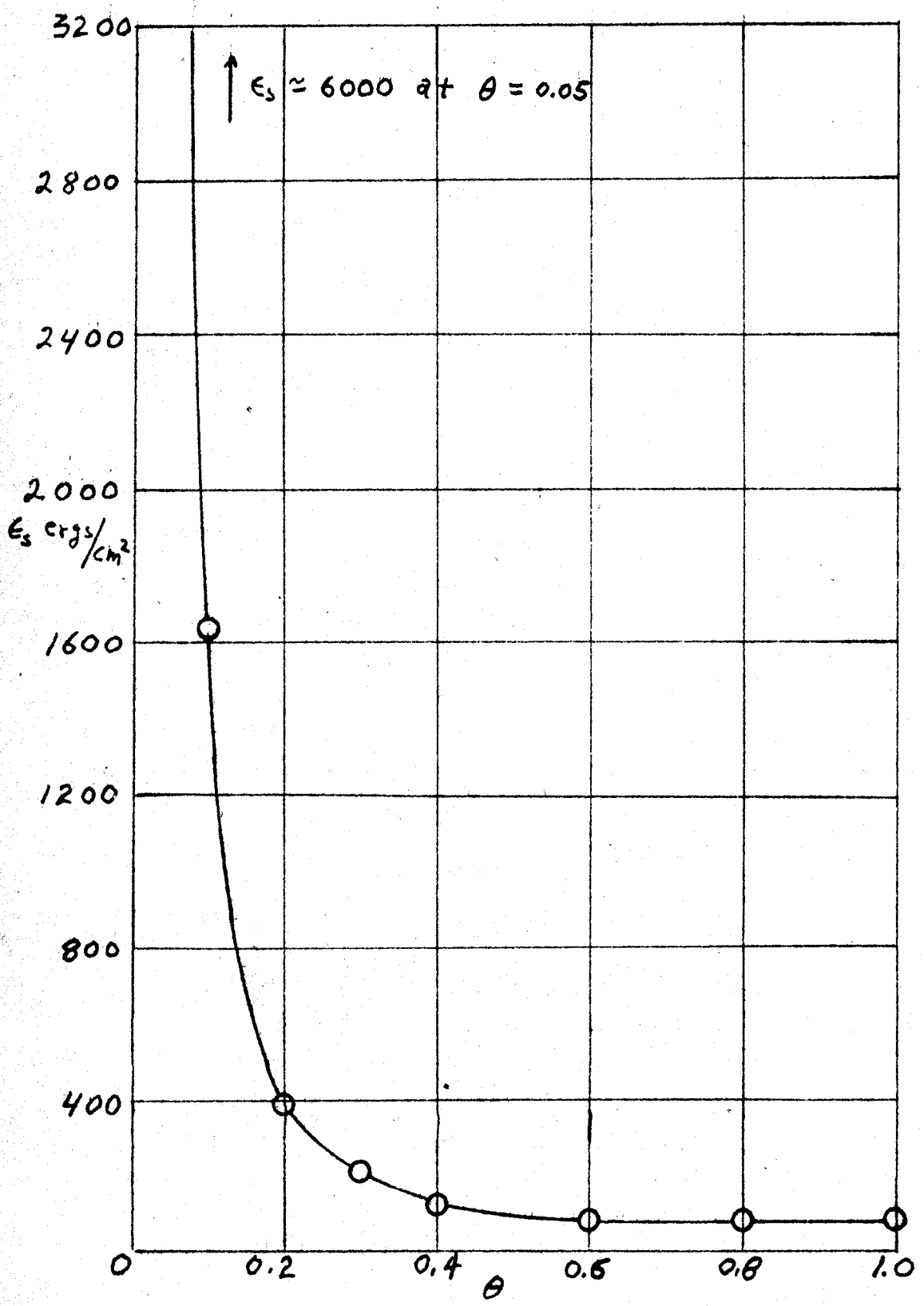

A theory has been developed that makes possible the calculation of the energy of adhesion of ice to solids from heat of wetting and adsorption data. Experiments were performed on six different solids, and the energy of ice adhesion calculated for them. The results of these calculations were consistent with known facts. A specific check of the data with the literature was not possible since no adhesion energy values for solid-solid systems have been reported.

Several approximate relations between surface quantities arise from the theory, that could be checked with known experimental data. These equations include surface energy, surface tension, and contact angle relations. All of these gave reasonable agreement with experiments.

A method has also been developed for investigating surface heterogeneity and determining the distribution function for the energy over a surface. The above mentioned theory was used to compute this distribution function from the heat of wetting as a function of preadsorbed material. The results of these measurements indicate that the two surfaces investigated, lead chromate and aluminum oxide, are quite heterogeneous. Only about 30% of the available surface contributes to the high energy surface properties of

these substances, the remaining 70% having relatively low energy.

Although experimental and computational difficulties make this work somewhat approximate, the results are thought to be of great value. These data represent the first adhesion energies measured for solid-solid systems, and the first direct measure of the heterogeneity of surfaces in regard to their energy.

BIBLIOGRAPHY

1. Kraus, Gerard. Progress Report No. 2 (Nov. 1 - Feb. 1, 1952-53) Army Air Force Contract AF 33 (616) 231, University of Cincinnati.

2. Fowler, R., and Guggenheim, E. A. "Statistical Thermodynamics." Cambridge University Press (1949) Ch. X.

3. Harkins, W. D., and Jura, G. "The Surfaces of Solids and Liquids and the Films that Form upon Them," in "Colloid Chemistry." Vol. VI, p. 1-76, edited by J. Alexander. Reinhold Publishing Corp. New York (1946).

4. Bangham, D. H., Trans. Farad. Soc., 33, 805 (1937).

5. Bangham, D. H., and Razouk, R. I., Trans. Farad. Soc., 33, 1463 (1937).

6. Bangham, D. H., and Razouk, R. I., Proc. Royal Soc. (London) A166, 572 (1938).

7. Brunauer, S. "The Adsorption of Gases and Vapors." Princeton University Press (1943). Ch. 8.

8. Fowler, R. "Statistical Mechanics." Cambridge University Press (1936). Ch. X.

9. Bikerman, J. J. "Surface Chemistry for Industrial Research." Academic Press Inc., New York (1948). Ch. V.

10. Drain, L. E., and Morrison, J. A., Trans. Farad. Soc., 48, 316 (1952).

11. Rhodin, T. N., J. Am. Chem. Soc., 72, 5691 (1950).

12. deBoer, J. H. "The Dynamical Character of Adsorption." Oxford Clarendon Press (1953). Ch. V.

13. Beattie, J. A., and Stockmayer, W. H. "The Thermodynamics and Statistical Mechanics of Real Gases" in "A Treatise on Physical Chemistry." Vol. II, Ch. II. Edited by H. S. Taylor and S. Glasstone. D. Van Nostrand Inc. New York (1951).

14. Slater, J. C. "Introduction to Chemical Physics." Ch. IX. McGraw-Hill Book Co. Inc. New York (1939).

15. Williams, J. W., and Alberty, R. A. "The Colloidal State and Surface Chemistry" in "A Treatise on Physical Chemistry." Vol. II, Ch. IV. Edited by H. S. Taylor and S. Glasstone. D. Van Nostrand Inc. New York (1951).

16. Harkins, W. D., A. A. A. S. Publication No. 21, 1 (1943).

17. Slater, J. C. "Introduction to Chemical Physics." Ch. XXII. McGraw-Hill Book Co. Inc. New York (1939).

18. Syrkin, Y. K., and Dyatkina, M. E. "Structure of Molecules and the Chemical Bond." Ch. 12. Interscience Publishers Inc. New York (1950).

19. Harkins, W. D. "Determination of Surface and Interfacial Tension" in "Physical Methods of Organic Chemistry." Vol. I. 2nd ed. Edited by A. Weissberger. Interscience Publishers Inc. New York

20. Hildebrand, J. H., and Scott, R. L. "Solubility of Non-Electrolytes." 3rd ed. Reinhold Publishing Corp. New York (1950).

21. Handbook of Chemistry and Physics. 30th edition. Chemical Rubber Publishing Co. (1947).

22. Donahue, D. J., and Bartell, F. E., J. Phys. Chem. 56, 480 (1952).

23. Adams, N. K. "Physics and Chemistry of Surfaces." 3rd ed. Oxford University Press (1941).

24. Ray, B. R., and Bartell, F. E., J. Coll. Sci. 8, 214 (1953).

25. Shafrin, E. G., and Zisman, W. A., J. Coll. Sci. 7, 166 (1952).

26. Baker, H. R., Shafrin, E. G., and Zisman, W. A., J. Phys. Chem. 56, 405 (1952).

27. Hare, E. F., Shafrin, E. G., and Zisman, W. A., J. Phys. Chem. 58, 236 (1954).

28. Scholberg, H. M., Guenther, R. A., and Coon, R. I., J. Phys. Chem. 57, 923 (1953).

29. Dundon, M. L., J. Am. Chem. Soc. 45, 2658 (1923).

30. Bartell, F. E., and Suggitt, R. M., J. Phys. Chem. 58, 36 (1954).

31. Lennard-Jones, J. E., and Taylor, H. S., Proc. Royal Soc. (London) A109, 476 (1925).

32. Dent, B. M., Phil. Mag. (7), 8, 530 (1929).

33. Beimuller, Zeit. F. Physik. 38, 759 (1936).

34. Jaeger, Zeit. Anorg. Chem. 101, 152 (1917).

35. Born, M., Ency. D. Math. Wiss. 5, 743 (1923).

36. Lipsett, S. G., Johnson, F. M. G., and Maass, O., J. Am. Chem. Soc. 49, 925 (1940).

37. Fricke, R., and Blaschke, F., Z. Elektrochem. 46, 46 (1940).

38. Jura, G., J. Chem. Phys. 12, 1335 (1949).

39. Fricke, R., and Dorger, Z. Anorg. Chem. 253, 2 (1945).

40. Fricke, R., and Meyer, F. R., Z. Phys. Chem. a181, 409 (1938).

41. Harkins, W. D., and Boyd, G. E., J. Am. Chem. Soc. 64, 1195 (1942).

42. Kraus, G., Fauser, D., and Berghausen, P., unpublished data (1951).

43. Il'in, B. V., and Kiselev, V. F., Doklady Akad. Nauk. 82, 85 (1952).

44. Boyd, G. E., A. A. A. S., Publication No. 21, 131 (1943).

45. Zettlemoyer, A. C., Young, G. J., Chessick, J. J. and Healey, S. H., J. Phys. Chem. 57, 649 (1953).

46. Howard, H. L., and Culbertson, J. L., J. Am. Chem. Soc. 72, 1185 (1950).

47. Il'in, B. V., Kiselev, V. F., Kiselev, Ya. E., Likhacheva, O. A., and Shcherbakova, K. D., Doklady Akad. Nauk. 75, 827 (1950).

48. Girifalco, L. A., and Paynter, D., unpublished data (1953).

49. Brunauer, S., Emmett, P. H., and Teller, E., J. Am. Chem. Soc. 60, 309 (1938).

50. Harkins, W. D., and Jura, G., J. Am. Chem. Soc. 66, 1366 (1944).

51. Kraus, G., Ross, J. W., and Girifalco, L. A., J. Phys. Chem. 57, 330 (1953).

52. Girifalco, L. A., M. S. Thesis, University of Cincinnati (1952).

53. Young, S. W., and Taylor, R. C., Anal. Chem. 19, 133 (1947).

54. Berghausen, P. Presented at Symposium on Adhesion, Case Institute of Technology, April (1952).

55. Fauser, D., M. S. Thesis, University of Cincinnati (1952)

56. Buelteman, H., M. S. Thesis, University of Cincinnati (1952).

57. Paynter, D., Ph. D. Thesis, University of Cincinnati (1954).